

Structure of Topological Lattice Field Theories in Three Dimensions

Stephen-wei Chung,[‡] Masafumi Fukuma,[#] and Alfred Shapere[‡]

Newman Laboratory of Nuclear Studies
Cornell University
Ithaca, N.Y. 14853-5001, USA

We construct and classify topological lattice field theories in three dimensions. After defining a general class of local lattice field theories, we impose invariance under arbitrary topology-preserving deformations of the underlying lattice, which are generated by two new local lattice moves. Invariant solutions are in one-to-one correspondence with Hopf algebras satisfying a certain constraint. As an example, we study in detail the topological lattice field theory corresponding to the Hopf algebra based on the group ring $\mathbf{C}[G]$, and show that it is equivalent to lattice gauge theory at zero coupling, and to the Ponzano-Regge theory for $G = \text{SU}(2)$.

May 1993

[‡] e-mail: chung@beauty.tn.cornell.edu

Address after Sep. 1, 1993: Fermi National Accelerator Laboratory,
P.O. Box 500, Batavia, IL 60510

[#] e-mail: fukuma@strange.tn.cornell.edu

Address after July 1, 1993: Yukawa Institute for Theoretical Physics,
Kyoto University, Kitashirakawa, Kyoto 606, Japan

[‡] e-mail: shapere@strange.tn.cornell.edu

1. Introduction

Topological field theories have played an important role in our attempts to understand the nonperturbative structure of string theory and quantum gravity. In three dimensions, for example, Witten's observation [1] that Einstein gravity can be recast as a topological field theory has provided us with a solvable model for testing hypotheses about more realistic theories of gravity. Three-dimensional Chern–Simons–Witten (CSW) theories have been useful in understanding and systematizing two-dimensional conformal field theories [2] and integrable models [3], and even appear in formulations of open string field theory [4].

Mathematicians have also found topological field theories (TFTs) to be valuable tools, particularly in the study of topological invariants of manifolds. For example, CSW theories, in addition to their physical applications, generate Jones polynomials and other invariants of three-manifolds as correlation functions [5]. Similarly, Donaldson polynomials are generated by a four-dimensional topological gauge theory [6], and topological gravity in two dimensions models intersection theory on the moduli space of Riemann surfaces [7,8].

As the list of topological field theories and their applications continues to grow, so does the need for an axiomatic, constructive description of them. In fact, TFTs are so highly constrained by their symmetry that it does not seem unrealistic to hope that such a description could lead to a classification of TFTs, or at least to the discovery of new ones.

The usual description of topological field theories, in terms of continuum path integrals, possesses the merits of manifest symmetry and a straightforward semiclassical limit. However, path integral field theories contain an infinite number of degrees of freedom, almost all of which must be gauge-fixed or cancelled in order to obtain a TFT. Another difficulty of the path integral approach is its lack of mathematical rigor. Perhaps a simpler formulation, without spurious degrees of freedom and without divergences, would facilitate the systematic construction and classification of topological field theories.

The lattice approach to defining quantum field theories rigorously is well-established in many contexts. Usually, the lattice definition of a quantum field theory requires a continuum limit to be taken, and to find the appropriate continuum limit is one of the major tasks in the lattice construction. However, if the lattice theory is topological, then all lattice scales are equivalent — provided the lattice is fine enough to contain all the topological information about the underlying manifold — and in particular, the lattice theory is formally *equivalent* to its continuum limit. By putting TFTs on the lattice,

calculations of physical quantities are reduced to combinatorics, no spurious states appear, and, as we aim to show in this paper, the underlying geometric and algebraic structures are greatly clarified.

Our general method for constructing TFTs on the lattice will be as follows. First we recall that TFTs are continuum field theories invariant under arbitrary smooth, *local* deformations of the background metric. In such theories, physical quantities depend only on the topology of the underlying manifold, and not on its local geometry. Likewise, a lattice field theory is said to be topological if it is invariant under arbitrary local deformations of the underlying lattice. Thus, in a “topological lattice field theory” (TLFT), physical quantities will depend on the lattice only through its topology. To find a useful criterion for topological invariance, we first look for a simple set of lattice moves that generate all local topology-preserving deformations. Then, to prove that a given lattice theory is topological, it suffices to show that its partition function is invariant under these generating moves.

Two-dimensional TLFTs were constructed and extensively studied in refs. [9,10,11,12] according to the above procedure. As will be reviewed in section 2, only two local moves are needed to generate all topologically equivalent simplicially triangulated lattices in two dimensions: the bond flip and the bubble move [12,13,14]. Lattice theories invariant under these moves, *i.e.* 2D TLFTs, are in one-to-one correspondence with semisimple associative algebras. The construction is quite general; in fact, all known topological matter theories in two dimensions (*e.g.* 2D topological Yang-Mills theory [15] and twisted $N = 2$ minimal topological matter [16]) are obtained from TLFTs of this sort [11,12].

The first three-dimensional TLFT was constructed by Ponzano and Regge in 1967 [17], motivated by the so-called Regge calculus of 3D quantum gravity. In their model, a tetrahedral lattice is chosen, and each edge of the lattice is assigned an irreducible representation of $SU(2)$, so that a $6j$ -symbol of $SU(2)$ can be uniquely determined for each tetrahedral cell. The partition function is the sum over irreducible representations of the product over all tetrahedra of these $6j$ -symbols, and is shown to be invariant under a set of local moves that generate all local deformations of the tetrahedral lattice, namely, barycentric subdivision and a move that transforms two adjacent tetrahedra into three. Turaev and Viro [18] (see also [19,20,21,22]) generalized to models involving $6j$ -symbols for the quantum group $SU_q(2)$, and Dijkgraaf and Witten [23] constructed models based on discrete groups. Subsequently, Turaev [24], and Ooguri and Sasakura [25] proved that the

Ponzano–Regge model is equivalent to the CSW theory with gauge group $\text{ISO}(3)$. These constructions of 3D TLFTs are strongly based on the properties of group (or quantum group) representations, and moreover, they are only applicable to tetrahedral lattices. Thus, they do not seem to encompass all consistent 3D TFTs.

Our main goal in this paper is to give an alternative (and hopefully more general) approach to 3D TLFTs, with emphasis on the parallels of our construction with the construction of 2D TLFTs of refs. [11,12]. In particular, we will show that our 3D TLFTs are in one-to-one correspondence with a class of Hopf algebras.

The present paper is organized as follows.

In section 2, we will review the basic structure of 2D TLFTs [11,12] from a point of view that will carry over in subsequent sections to higher-dimensional TLFTs.

In section 3, we will present a systematic construction of 3D TLFTs, defined not only on tetrahedral lattices, but on arbitrary 3D cell complexes as well. As in two dimensions, topological invariance is implemented by a reduced set of two local lattice moves, which are sufficient to generate all topologically equivalent lattices. If we were interested only in tetrahedral lattices, then the two tetrahedral moves mentioned above would be sufficient. However, in order to account for arbitrary topologically equivalent lattices, we will introduce a more powerful set of moves, to be called the “hinge” and “cone” moves, which actually generate all local deformations of the lattice, including the original tetrahedral moves. (The bulk of the proof of this statement is contained in Appendix B.) Our construction of 3D TLFTs amounts to imposing invariance under these two new local moves.

Extending the program of refs. [11,12] to three dimensions, we will give our construction an algebraic interpretation, and show how to associate to each lattice theory an algebraic structure. The structure includes a multiplication operation, defined on faces, and a comultiplication, defined on hinges (edges). Reinterpreted in algebraic terms, the condition of invariance under the hinge and cone moves will be shown to imply that the multiplication and comultiplication operations must satisfy the axioms of a Hopf algebra, with an additional constraint on the antipode. (A brief review of Hopf algebras is given in Appendix A.) Furthermore, these constrained Hopf algebras will be shown to be in one-to-one correspondence with 3D TLFTs.

In section 4, we will recover the original model of Ponzano and Regge as a special case of our construction, with Hopf algebra based on the group ring of $\text{SU}(2)$. In addition, we will show that this model is equivalent to $\text{SU}(2)$ lattice gauge theory at zero coupling.

Finally, in section 5, we will offer some speculations on the relationship of our TLFTs to other TFTs, and discuss generalizations to higher dimensions.

2. Two-Dimensional Topological Lattice Field Theories

Our study of topological lattice models begins in two dimensions. Recently, two-dimensional topological lattice field theories were shown to be in one-to-one correspondence with semisimple associative algebras [11,12]. In this section we will review the definition and classification of these models, from a point of view that will carry over in subsequent sections to higher-dimensional TLFTs.

2.1. Definitions

By a two-dimensional lattice, we mean a collection of polygons with edges identified pairwise. We will assume for now that the lattice is without boundary, *i.e.*, that all edges are paired. We will also assume that the lattice contains only triangular faces. Both of these assumptions will be relaxed below.

A coloring of a lattice L associates to each edge of each triangle in L , an element x of an index set X . A lattice field theory (LFT) is defined by specifying a rule for assigning a weight to each possible coloring $\{x\}$. The partition function of the LFT is a weighted sum over all possible colorings.

To be more specific, we will consider a class of theories in which the weighting rule is defined locally on individual triangles, and compute the overall weight by multiplying the local weights of all the triangles together. Thus to each triangle Δ , with edges colored by x , y , and z , we assign a complex number $C_{xyz}(\Delta)$. Since there is no canonical ordering of the edges on Δ , it is natural to impose cyclic symmetry on the C_{xyz} ;

$$C_{xyz} = C_{yzx} = C_{zxy}. \quad (2.1)$$

We will not, however, assume any relation between C_{xyz} and the orientation-reversed C_{yxz} .

The operation of identifying edges of adjacent triangles is effected by means of a “gluing operator” on the space X , which we denote by g^{xy} . For the configuration depicted in Fig. 2-1 consisting of two adjacent triangles, the associated weight is

$$C_{xyu} g^{uv} C_{vzw} \equiv C_{xy}{}^u C_{uzw}, \quad (2.2)$$

where as usual all repeated indices are summed over, and indices of C_{xyz} are raised by contracting with the gluing operator.

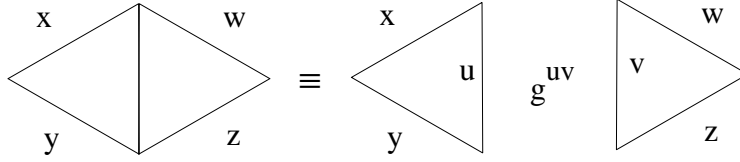


Fig. 2-1: Two adjacent triangles.

With these conventions, the partition function of the LFT on a given triangular lattice L is

$$Z(L) \equiv \prod_{\Delta \in L} \prod_{\langle uv \rangle} C_{xyz}(\Delta) g^{uv}, \quad (2.3)$$

where the second product is over all pairs of identified edges. For a lattice without boundary, the indices on all edges should be contracted.

2.2. Topological Invariance

We would now like to find a set of conditions under which the partition function (2.3) is invariant under local changes of the lattice L .

It is a theorem of Alexander that all triangulations of a topological manifold can be generated by a set of local topology-preserving lattice moves [26]. One formulation of Alexander's theorem [13,14,18,12] says that just two basic moves are sufficient to generate all topologically equivalent two-dimensional triangular lattices. The first move, which flips an edge between two adjacent triangles, is called the (2,2) move, because it converts two triangles into two new triangles, as shown in Fig. 2-2a. The second move, called the bubble move and drawn in Fig. 2-2b, collapses a pair of triangles with two edges in common to a single edge. According to the theorem, a lattice field theory, whose partition function is invariant under both (2,2) and bubble moves, is invariant under any local changes of triangulation, and thus depends only on the topology of the underlying lattice. This is the defining property of a topological lattice field theory.

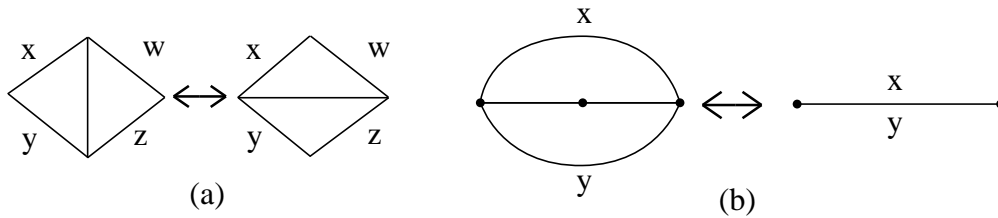


Fig. 2-2: (2,2) move and bubble move.

For the type of lattice field theory represented in eq. (2.3), topological invariance has a simple expression in terms of the weights C_{xyz} and the gluing operator g^{xy} . Invariance under the (2,2) move implies that

$$C_{xy}^u C_{uz}^w = C_{xu}^w C_{yz}^u, \quad (2.4)$$

where we have raised the index w for later convenience. Likewise, invariance under the bubble move is equivalent to

$$C_{xu}^v C_{yv}^u = g_{xy}, \quad (2.5)$$

where g_{xy} is the matrix inverse of the gluing operator g^{xy} , and will be called the “metric.”

Equations (2.4) and (2.5) are necessary and sufficient conditions for an LFT defined by the data (C_{xyz}, g^{xy}) to have topological invariance. As such, they may be taken as the defining equations of a two-dimensional TLFT. Before proceeding with their interpretation and solution, we would like to make the following remarks.

- (I) (2,2) invariance (eq. (2.4)) and bubble invariance (eq. (2.5)) lead to the following equation

$$C_{xy}^v C_{vu}^u = g_{xy}. \quad (2.6)$$

This equation guarantees invariance under the “cone move,” which transforms the cone-like configuration of two triangles in Fig. 2-3a into a single edge in Fig. 2-3b. (For the sake of clarity, two additional triangles C_{xab} and C_{ycd} are attached to the edges x and y in Fig. 2-3c.) Fig. 2-4 gives a graphical proof of eq. (2.6), and also shows that, conversely, the cone move and the (2,2) move generate the bubble move; hence, the cone and (2,2) moves are an alternative set of moves that generate all topology-preserving deformations.

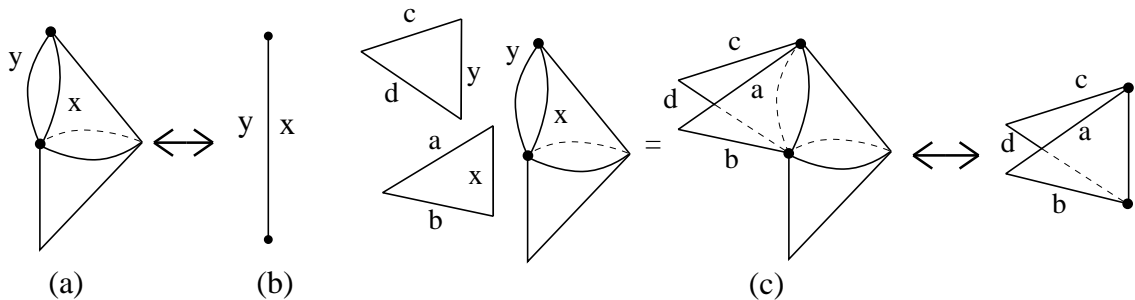


Fig. 2-3: Cone move.

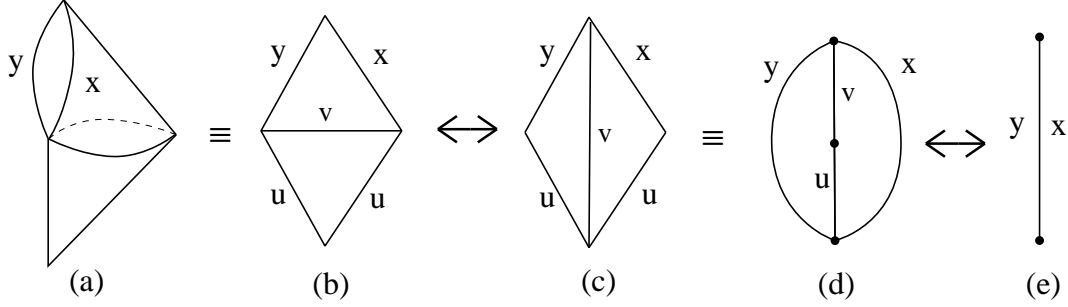


Fig. 2-4: Cone move from bubble move.

- (II) The (2,2) and bubble moves can actually be interpreted as lattice analogues of local metric deformations in continuum. In fact, the (2,2) move, which preserves locally the number of triangles, is a lattice analogue of an area-preserving diffeomorphism. The bubble move decreases the number of triangles in a local region of the lattice; it is like a Weyl transformation. In continuum, it is well-known that area-preserving diffeomorphisms and Weyl transformations generate all local deformations of metric. The corresponding statement here is that (2,2) and bubble moves generate all local topology-preserving deformations of a triangular lattice. It is also interesting to study lattice theories invariant under only (2,2) or bubble transformations. For example, two-dimensional lattice gauge theory can be shown to be invariant under the (2,2) move, corresponding to its invariance under area-preserving diffeomorphisms in continuum [15,27].
- (III) Up to now, we have considered only triangular lattices. With little additional effort, we can relax this assumption, and extend our arguments to lattices with non-triangular as well as triangular faces. To define a general LFT on such a lattice, we need to introduce an infinite set of new weights $C_{x_1 \dots x_n}$, in order to account for the contribution of an arbitrary n -gon. Now the topology-preserving moves that we have defined so far are sufficient to relate all topologically equivalent triangular lattices; however, to obtain all topologically equivalent lattices with general polygonal faces as well, we must consider additional moves that generate subdivisions of polygons into triangles. After imposing subdivision invariance on the generalized weights $C_{x_1 \dots x_n}$, we find that they are completely determined by the old, triangular weights, since n -gons can always be decomposed into triangles; for the decomposition shown in Fig. 2-5, we obtain

$$C_{x_1 \dots x_n} = C_{a_1 x_1 b_1} g^{b_1 a_2} C_{a_2 x_2 b_2} g^{b_2 a_3} \dots C_{a_n x_n b_n} g^{b_n a_1} . \quad (2.7)$$

Topological invariance guarantees that the generalized weights so obtained are well-defined, that is, independent of the triangular decomposition chosen. Because all higher weights are completely determined by the original triangular weights, no new topological field theories are obtained by considering arbitrary polygonal lattices, and 2D TLFTs on arbitrary lattices are in one-to-one correspondence with solutions to the (2,2) and bubble equations, eqs. (2.4) and (2.5).

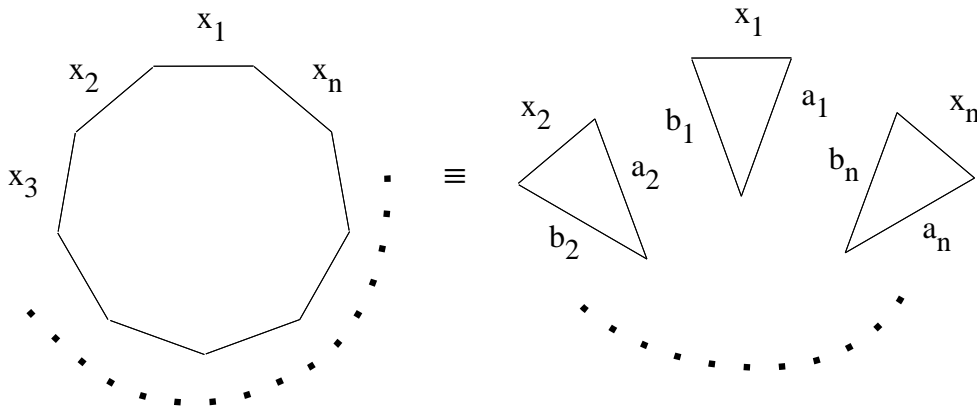


Fig. 2-5: A decomposition of an n -gon.

2.3. Algebraic Structure

We will now explain how a solution (C_{xyz}, g^{xy}) to the (2,2) and bubble equations, besides defining a TLFT, also determines an algebraic structure. Namely, we will review that given any two-dimensional TLFT, we can construct a semisimple associative algebra [11,12].

The algebra in question is defined on the the vector space A over \mathbf{C} generated by the index set X :

$$A = \bigoplus_{x \in X} \mathbf{C} \phi_x . \quad (2.8)$$

We introduce a multiplication operation on A , by means of the $C_{xy}{}^z \equiv C_{xyz'} g^{z'z}$:

$$\phi_x \cdot \phi_y \equiv C_{xy}{}^z \phi_z . \quad (2.9)$$

Then it is easy to see that eq. (2.4) – invariance under the (2,2) move – is equivalent to the associativity of the multiplication [11,12]:

$$(\phi_x \cdot \phi_y) \cdot \phi_z = \phi_x \cdot (\phi_y \cdot \phi_z) . \quad (2.10)$$

Furthermore, in the bubble equation (2.5), we implicitly assume that the inverse of g_{xy} exists, which is the gluing operator g^{xy} . Note here that the nondegeneracy of g_{xy} is equivalent to the condition that A be semisimple [12]. Thus, given a topologically invariant lattice field theory, defined by data C_{xyz} and g^{xy} satisfying (2.4) and (2.5), we can always construct a semisimple associative algebra.

Conversely, a TLFT can be constructed from a given semisimple associative algebra on a vector space A with structure constants $C_{xy}{}^z$ [11,12]. By applying the quadratic form $g_{xy} = C_{xu}{}^v C_{yv}{}^u$ to the structure constants, we construct a set of triangular weights $C_{xyz} \equiv C_{xy}{}^{z'} g_{z'z}$, which can be shown to be cyclic by using the associativity condition (2.4). The semisimple condition implies that the matrix inverse g^{xy} of g_{xy} exists; this is our gluing operator. Since the LFT data C_{xyz} and g^{xy} satisfy eqs. (2.4) and (2.5) by assumption, they automatically define a TLFT.

In summary, we have shown

Theorem 2.1. [11,12] *Two-dimensional topological lattice field theories are in one-to-one correspondence with semisimple associative algebras.*

We close this subsection with a remark on the algebraic interpretation of the “cone equation” (2.6): in a 2D LFT whose gluing operator has its inverse, invariance under the cone move is equivalent to the existence of a unit element 1_A in the corresponding algebra A . In fact, by rewriting eq. (2.6) in the form

$$u^x C_{xy}{}^z = \delta_y^z = u^x C_{yx}{}^z \quad (2.11)$$

with $u^x \equiv g^{xy} C_{yu}{}^x$, we obtain an equation equivalent to the defining property of a unit element $1_A \equiv u^x \phi_x$ of A :

$$1_A \cdot \phi = \phi = \phi \cdot 1_A, \quad \forall \phi \in A. \quad (2.12)$$

This result corresponds to the mathematical fact that in any semisimple associative algebra, we can uniquely introduce a unit element 1_A of the above form (see Theorem A.1).

2.4. Physical Observables

Our main concern up to now has been the definition of partition functions with topological invariance. We will now describe how to construct physical operators and states.

A natural operator to consider is the operator $\mathcal{O}_{xyz}(\Delta)$ that fixes the colors x , y , and z on the edges of a single triangle Δ . The formal definition of this operator, which is conjugate to $C^{xyz}(\Delta)$, is

$$\mathcal{O}_{xyz}(\Delta) = \frac{\delta}{\delta C^{xyz}(\Delta)}, \quad (2.13)$$

so that correlation functions are given by

$$\langle \mathcal{O}_{x_1 y_1 z_1}(\Delta_1) \cdots \mathcal{O}_{x_k y_k z_k}(\Delta_k) \rangle = \frac{\delta}{\delta C^{x_1 y_1 z_1}(\Delta_1)} \cdots \frac{\delta}{\delta C^{x_k y_k z_k}(\Delta_k)} Z. \quad (2.14)$$

The insertion of an operator $\mathcal{O}_{xyz}(\Delta)$ causes the sum over colorings of the lattice to be restricted to those colorings that have the fixed values x , y , and z on the edges of Δ , and removes the weighting factor C^{xyz} of the triangle Δ from the partition function (2.3). $\mathcal{O}_{xyz}(\Delta)$ thus effectively punches a triangular hole in the lattice with boundary Δ and boundary values x , y , and z . We can further construct an operator that creates an arbitrary polygonal boundary by gluing triangular operators \mathcal{O}_{xyz} together and summing over glued edges. For example, if Δ_1 and Δ_2 are two adjacent triangles making up a quadrilateral \square with edges x , y , z , and w , then we can define $\mathcal{O}_{xyzw}(\square)$ as

$$\mathcal{O}_{xyzw}(\square) \equiv \frac{\delta}{\delta C^{xyzw}} = \mathcal{O}_{xy}{}^u(\Delta_1) \mathcal{O}_{uzw}(\Delta_2). \quad (2.15)$$

The colorings of a fixed boundary created by the operators $\mathcal{O}_{x_1 x_2 \dots x_n}$ are naturally regarded as forming a Hilbert space of states. In order to determine which of these states are physical, we introduce the following ‘‘Hamiltonian formalism’’ (following ref. [28]).¹ First, we give a more precise definition of the Hilbert space \mathcal{H}_B (not necessarily physical) as the module freely generated by all possible colorings C of a ‘‘triangulated’’ one-dimensional closed manifold B . Thus, a wave function in \mathcal{H}_B is a complex-valued function of a coloring on B ; $\mathcal{H}_B = \{\Phi_B(C)\}$. We then define the ‘‘time’’-evolution kernel $P_{B',B}(C', C)$, which maps a state $\Phi_B(C)$ in \mathcal{H}_B to a state $\Phi_{B'}(C')$ in $\mathcal{H}_{B'}$, as the cylinder with boundary $B' \cup (-B)$. Here, $-B$ denotes the orientation reverse of B . In a topological theory, the

¹ An alternative approach is given in ref. [12].

cylinder $P_{B',B}(C', C)$ should be independent of its triangulation; in particular it should obey the composition law

$$P_{B'',B}(C'', C) = \sum_{C'} P_{B'',B'}(C'', C') P_{B',B}(C', C) \quad (2.16)$$

for arbitrary intermediate boundary B' . Taking $B = B' = B''$ in (2.16), we see that $P_{B,B}^2 = P_{B,B}$, *i.e.*, the cylinder $P_{B,B}$ is a projection operator. Physical states $\Psi_B(C)$, which appear on the intermediate slice $B' = B$, can be characterized by their invariance under “time”-evolution by $P_{B,B}$:

$$\Psi_B(C') = \sum_C P_{B,B}(C', C) \Psi_B(C) . \quad (2.17)$$

$P_{B,B}$ is thus the projection operator of \mathcal{H}_B onto the physical Hilbert space $\mathcal{H}_B^{\text{phys}}$, and is the propagator of physical states.

For example, let us determine the physical states on a lattice with a boundary consisting of a single edge, with coloring x . The projection operator should correspond to a cylinder with two one-gonal holes, with colorings x and y . Such a cylinder can be triangulated as in Fig. 2-6, and from this triangulation we determine that the propagator is

$$P_x^y = C_{xu}^v C_v^{yu} . \quad (2.18)$$

This is precisely the projection operator onto one-gonal physical states that was found in ref. [12] (where it is called η_x^y). There, it was further shown that P_x^y is algebraically a projection operator from the semisimple associative algebra A onto its center $Z(A)$, and that there is a one-to-one correspondence of elements of $Z(A)$ with physical operators.

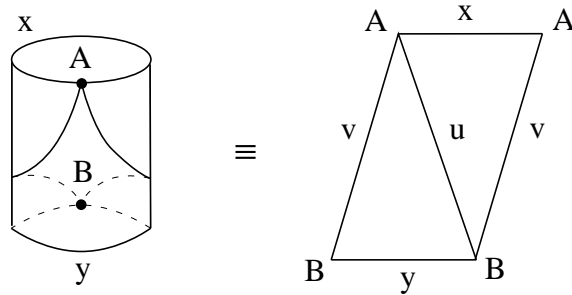


Fig. 2-6: A triangulation of a cylinder with two one-gonal holes, x and y .

Besides the propagator, we can define an interaction vertex for physical states in terms of the 3–point function of 3 separated one–gons shown in Fig. 2-7:

$$N_{xyz} \equiv P_x^p P_y^q P_z^r C_{pqr} = P_x^p P_y^q P_z^r C_{qpr} = N_{yxz} . \quad (2.19)$$

Eq. (2.19) implies that N_{xyz} is the totally symmetric projection of C_{xyz} to $Z(R)$. These data P and N are sufficient to calculate all correlation functions of physical operators of arbitrary genus.

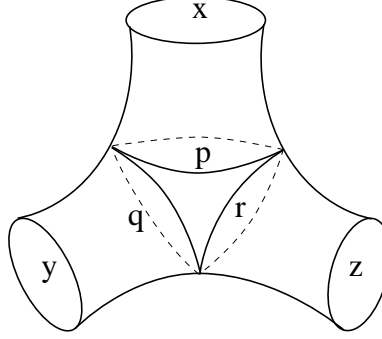


Fig. 2-7: Three-point function of \mathcal{O}_x , \mathcal{O}_y , and \mathcal{O}_z .

2.5. Example: $A = \mathbf{C}[G]$

A simple example of an associative algebra is provided by group ring $A = \mathbf{C}[G] = \bigoplus_{x \in G} \mathbf{C} \phi_x$, with multiplication inherited from the group G , $\phi_x \cdot \phi_y = \phi_{xy}$. Let $\int dx$ be its normalized Haar measure:

$$\begin{aligned} \int d(gxh) &= \int dx & (\forall g, h \in G) \\ \int dx \, 1 &= 1 . \end{aligned} \quad (2.20)$$

Associated with this Haar measure is the left–right invariant δ -function $\delta(x, y)$:

$$\begin{aligned} \int dy \, \delta(x, y) f(y) &= f(x) \\ \delta(gxh, gyh) &= \delta(x, y) , & (\forall x, y, g, h \in G) . \end{aligned} \quad (2.21)$$

For a finite group G , we define the measure and δ -function by ²

$$\begin{aligned} \int dx &\equiv \frac{1}{|G|} \sum_{x \in G} \\ \delta(x, y) &\equiv |G| \delta_{x,y} . \end{aligned} \quad (2.22)$$

² In ref. [12], $\delta_{x,y}$ is denoted by $\delta(x, y)$.

The structure constants for $A = \mathbf{C}[G]$ are thus

$$C_{xy}{}^z = \delta(xy, z) . \quad (2.23)$$

Following eq. (2.5) we have

$$\begin{aligned} g_{xy} &= C_{xu}{}^v C_{yv}{}^u = \int du dv \delta(xu, v) \delta(yv, u) = \delta(x, y^{-1}) \\ C_{xyz} &= C_{xy}{}^u g_{uz} = \int du \delta(xy, u) \delta(u, z^{-1}) = \delta(xyz, 1_G) . \end{aligned} \quad (2.24)$$

Now we can readily calculate the two- and three-point functions of one-gons on the sphere, using the same triangulations as in eqs. (2.18) and (2.19):

$$\begin{aligned} P_{xy} &= C_{xu}{}^v C_{vy}{}^u = \int du dv \delta(xu, v) \delta(vy, u) = \int dv \delta(x, vy^{-1}v^{-1}) = \delta_{[x],[y^{-1}]} \\ &= \sum_j \chi_j(x) \chi_j(y) \\ N_{xyz} &= \int dx' dy' dz' P_x^{x'} P_y^{y'} P_z^{z'} \delta(x'y'z', 1_G) = \sum_j \frac{\chi_j(x) \chi_j(y) \chi_j(z)}{d_j} , \end{aligned} \quad (2.25)$$

where $[x]$ denotes the conjugacy class of x , and, χ_j and d_j are, respectively, the group character and the dimension of an irreducible representation j . By iteration, the correlation function for n one-gons on genus g can be computed to be [27,11,12]

$$\langle \mathcal{O}_{x_1} \mathcal{O}_{x_2} \cdots \mathcal{O}_{x_n} \rangle_g = \sum_j \frac{\chi_j(x_1) \chi_j(x_2) \cdots \chi_j(x_n)}{d_j^{n+2g-2}} . \quad (2.26)$$

Arbitrary correlation functions of the p -gon operators $\mathcal{O}_{x_1 \cdots x_p}$ can easily be computed as well, and are no more complicated than correlation functions of one-gons. In fact, we only have to connect a cylinder with two boundary loops, one of which is one-gonal, and the other is p -gonal. For example, in the case of $p = 2$, we attach one edge of a triangle, with free edges y and z forming a two-gon, to a cylinder with one-gon ends, as in Fig. 2-8. The result is simply

$$\langle \mathcal{O}_x \mathcal{O}_{yz} \rangle_{g=0} = P_x^{x'} C_{x'yz} = P_{x,yz} = \sum_j \chi_j(x) \chi_j(yz) . \quad (2.27)$$

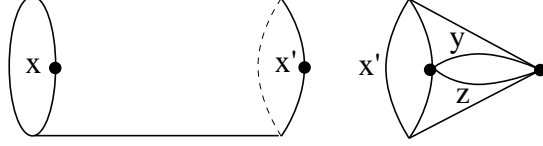


Fig. 2-8: Two point-function of \mathcal{O}_x and \mathcal{O}_{yz} .

Similarly, we have the following expression for arbitrary p_i :

$$\langle \mathcal{O}_x \mathcal{O}_{y_1 \cdots y_p} \rangle_{g=0} = P_{x, y_1 \cdots y_p} = \sum_j \chi_j(x) \chi_j(y_1 \cdots y_p). \quad (2.28)$$

By attaching two-point functions of the form (2.28) to one-gonal correlation functions such as (2.26), we can build any correlation function of p -gonal operators. The result is of the same form as eq. (2.26), but with x_i replaced by the product of group elements around the i th polygon:

$$\begin{aligned} & \langle \mathcal{O}_{x_{(1,1)}, \dots, x_{(1,p_1)}} \cdots \mathcal{O}_{x_{(n,1)}, \dots, x_{(n,p_n)}} \rangle_g \\ &= \sum_j \frac{\chi_j(x_{(1,1)} \cdots x_{(1,p_1)}) \cdots \chi_j(x_{(n,1)} \cdots x_{(n,p_n)})}{d_j^{n+2g-2}}, \end{aligned} \quad (2.29)$$

where $x_{(i,j)}$ is the group element on the j th edge of the i th polygon.

2.6. Dual Formulation

There is an equivalent approach to constructing TLFTs, in which interactions take place at vertices instead of on triangles. For simplicity, but ultimately without loss of generality, we will suppose that all vertices are trivalent. Then given a lattice whose links form a trivalent graph, we can construct a lattice field theory by gluing all the vertices together. The weight Δ^{xyz} of a vertex will depend on the colorings of the three lines emanating from it, and vertices will be glued using a two-indexed operator h_{xy} . Similarly to eq. (2.3), the partition function of this theory will be the product of all vertex weights Δ^{xyz} , with all indices contracted using h_{xy} .

Of course, this lattice model is completely dual to our previous construction, and is in all respects mathematically equivalent, but it may be instructive to review the axioms of topological invariance in this framework. For this purpose, we may replace any of our previous pictures of triangles glued together along links, by dual graphs, in which dual

vertices are connected by dual links. Then (2,2) invariance (eq. (2.4)) of the original lattice theory is now expressed as

$$\Delta_x^{yu} \Delta_u^{zw} = \Delta_x^{uw} \Delta_u^{yz} \quad (2.30)$$

in this dual picture (see Fig. 2-9a). Furthermore, we can consider the “dual bubble move,” that is, the move in the dual lattice corresponding to the bubble move in the original lattice,

$$h^{xy} = \Delta_u^{vx} \Delta_v^{uy}, \quad (2.31)$$

from whose graphical expression (Fig. 2-9b) the bubble move derives its name.

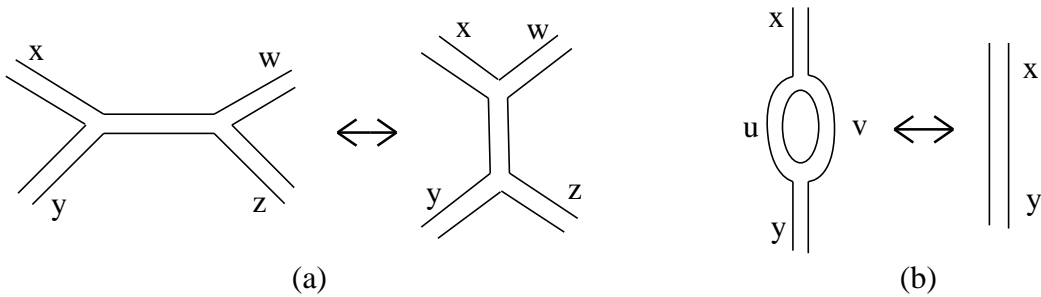


Fig. 2-9: Dual diagrams of Fig. 2-2.

We may also consider lattice theories containing both C_{xyz} 's and Δ^{xyz} 's. In two dimensions, this just gives two uncoupled lattice models of the type we have already discussed. However, in the following section, an elaboration of this idea will form the basis for our construction of topological lattice theories in three dimensions.

3. Construction of TLFTs in Three Dimensions

In the previous section, we described a one-to-one correspondence between a class of 2D topological lattice field theories and semisimple associative algebras. Here we will show that in three dimensions there is a similar sort of correspondence between a class of TLFTs and a class of Hopf algebras. We begin by defining the class of lattice field theories (LFTs) of interest and establishing a diagrammatic representation for operations within these theories (subsec. 3.1). We then show that the data of these LFTs can be used to define algebra and coalgebra structures (subsec. 3.2). Our main result will be that these structures combine to form a special type of Hopf algebra if and only if the theory is invariant under arbitrary topology-preserving deformations of the lattice geometry (subsec. 3.3).

3.1. Definitions

In this subsection, we define a general class of lattice field theories in three dimensions, valid for an arbitrary lattice.

One possible way of describing a three-dimensional lattice L is as a collection of oriented polyhedra with faces glued pairwise. Such a lattice can be colored by associating to each of its edges an element x of an index set X . To define a local lattice field theory on L , we specify a rule that determines a local weight for each polyhedron, as a function of the colorings of its edges. The total weight of a given coloring is then computed by taking the product of the local weights of all polyhedral cells in L ; in turn, the partition function is defined to be the sum of these total weights over all allowed colorings.

This approach (especially for tetrahedral lattices) has formed the basis for most previous constructions of TLFTs in three dimensions [17,18,25,20]. However, we will find that the following alternative approach is better suited to our purpose of establishing a correspondence between TLFTs and algebraic structures.

We define a lattice L to be a collection of polygonal faces, with edges glued together – not necessarily pairwise – along one-dimensional hinges. We again color the lattice by associating to each edge of each face a color $x \in X$.³ As in two dimensions, the coloring of the boundary of each face determines a local weight. But in contrast to the two-dimensional case, in three dimensions it is possible for the edges of more than two faces to meet, as in Fig. 3-1a. We call a meeting of three or more edges a “hinge;” more precisely, a hinge is an open neighborhood of the line along which the faces meet. Hinges thus have edges that can be colored, and can be pictured as consisting of several infinitesimally thin strips emerging from a central line. For example, a four-valent hinge is contained in Fig. 3-1b. Because hinges, as well as faces, have edges that need to be colored and glued, a weighting rule for hinges must also be specified. This will be a function of the colors on the edges of the hinge, to be called the “hinge weight.”

³ Other coloring and weighting schemes are discussed in Sec. 5, as well as in ref. [22].

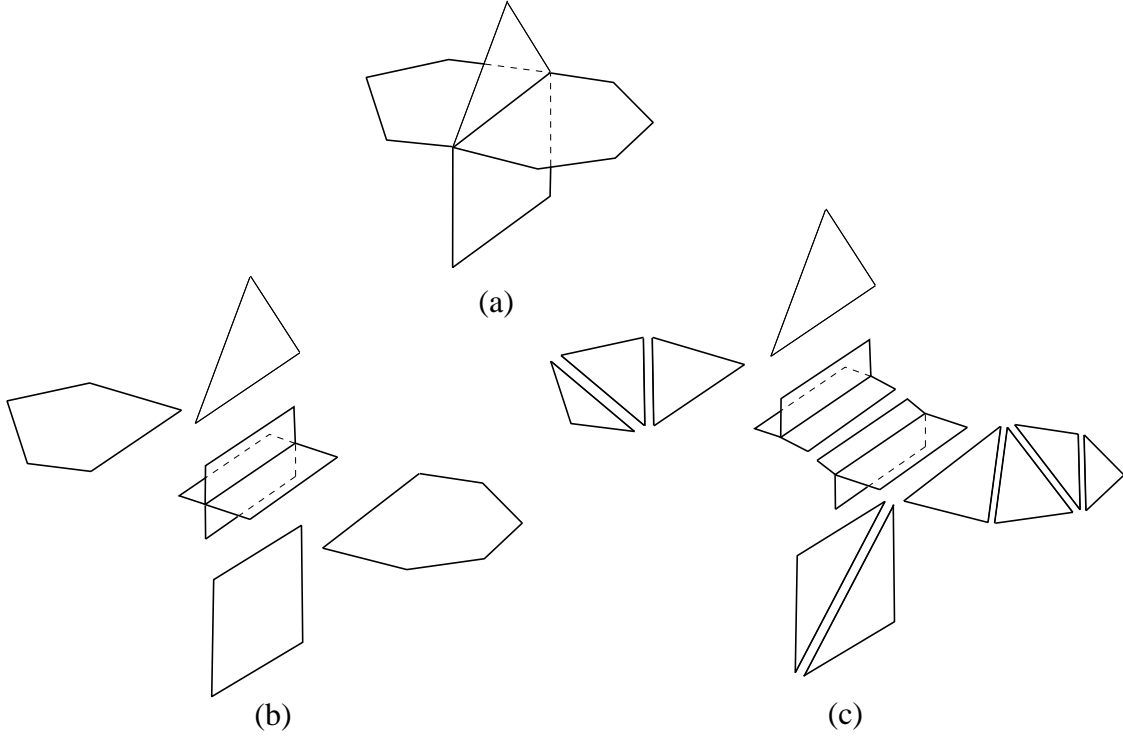


Fig. 3-1: The decomposition of a 3D lattice into faces and hinges.

The weighting rules for faces and hinges that we will consider will be of a particular type. Namely, we will further decompose, respectively, each polygonal face and each multivalent hinge into triangles and trivalent hinges (3-hinges), as depicted in Fig. 3-1c, and demand that our weighting rules be invariant under subdivision. This initial restriction, which is automatically satisfied in a topologically invariant theory, will not affect our conclusions with regard to 3D TLFTs, yet will greatly simplify the form of the weighting rules. Thus, in order to determine a complete set of weights for arbitrary faces and hinges, it will suffice to specify weights only for triangles and 3-hinges, and “gluing rules” that tell us how to connect triangles to triangles (so as to compute the weight of an arbitrary polygonal face in terms of triangular weights), and 3-hinges to 3-hinges (so as to compute the weight of an arbitrary multivalent hinge).

Besides weights for faces and hinges, we also have to specify how to connect faces to hinges, so as to form a 3D lattice. Since faces and hinges are already decomposed into triangles and 3-hinges, we only need to introduce additional gluing rules that tell us how to connect triangles to 3-hinges. Then, given this collection of triangles and 3-hinges, we define the partition function of our LFT to be the product of all triangle weights and 3-hinge weights, with color indices contracted according to the gluing rules.

We first define a weighting rule for triangular faces. To each triangle, whose three edges are colored by $x, y,$ and $z \in X$, we associate a complex number C_{xyz} . The weighting rule for faces is thus a map $C : X \times X \times X \rightarrow \mathbf{C}$. As in two dimensions, the symmetry of the triangle imposes cyclic symmetry on $C_{xyz} = C_{zxy} = C_{yzx}$. In order to keep track of the orientation of each triangle, we now draw arrows around its edges, as in Fig. 3-2.

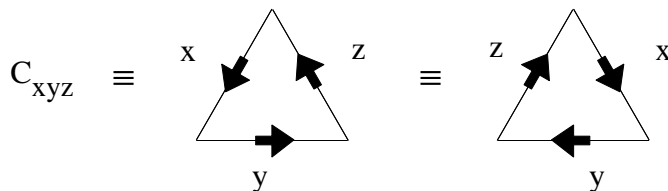


Fig. 3-2: Weight of a triangle C_{xyz} .

Similarly, we define a weighting rule for 3-hinges. A 3-hinge consists of three infinitesimally thin strips, as shown in Fig. 3-3a; its three outward edges are colored and will eventually be glued to faces (or to other hinges). For artistic convenience, we represent this hinge in Fig. 3-3b, as a diagram consisting of three parallel dotted lines with aligned arrows, labeled $x, y,$ and z . We assign a local weight Δ^{xyz} to the hinge, if the three edges meeting on the hinge have colors $x, y,$ and z . When the arrows on the parallel lines point upwards, our convention will be to orient $x, y,$ and z counterclockwise, viewed from above. Because none of the three faces is preferred, cyclic symmetry is also imposed: $\Delta^{xyz} = \Delta^{yzx} = \Delta^{zxy}$.

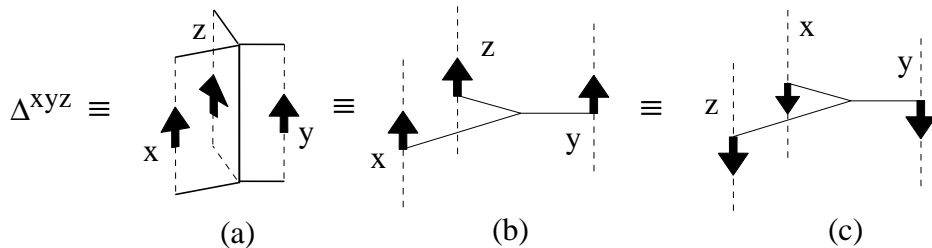


Fig. 3-3: Graphical representation of Δ^{xyz} .

Next, we will explain how to glue triangles to triangles and 3-hinges to 3-hinges.

To glue two edges of two triangular faces together, with colors x and y , we introduce a “face–gluing operator” g^{xy} . That is, we use g^{xy} to contract the indices of the triangular weights that correspond to the edges to be glued. We represent the operator g^{xy} by two parallel dotted lines, with arrows pointed in opposite directions, as in Fig. 3-4. In all of our diagrams, we will use dotted lines to represent raised indices and solid lines for lowered indices, with the rule that solid lines may only be glued to dotted lines, and then only if the arrows on the two lines have the same orientation. This rule is essentially the usual summation convention for repeated indices. For example, for the configuration of two triangles shown in Fig. 3-5, the corresponding local weight is $C_{xyu} g^{uv} C_{vzw} \equiv C_{xy}{}^u C_{uzw}$.

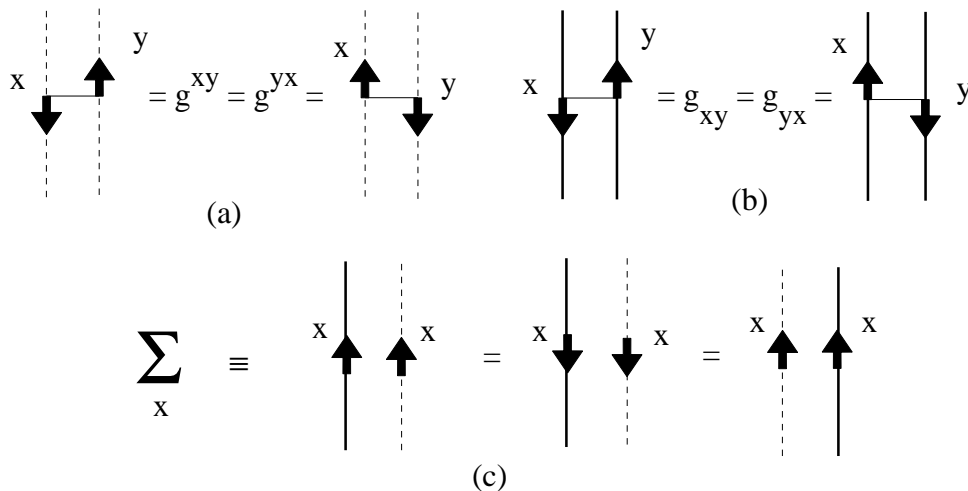


Fig. 3-4: Definitions of g_{xy} , g^{xy} and summation.

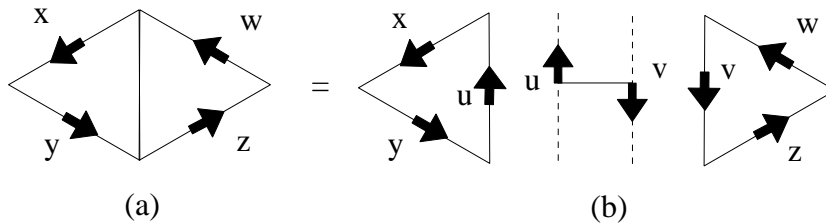


Fig. 3-5: Two triangles joined by g^{uv} .

Given a set of triangle weights C_{xyz} and gluing operators g^{xy} , we can now compute the weight of an arbitrary polygonal face, all of whose external edges are oriented in the

same direction (*i.e.*, clockwise or counterclockwise), by decomposing the polygon into a collection of triangles, similarly oriented. The weight of the polygonal face is defined to be the product of the local weights of the triangles, with all internal edge indices contracted using the face–gluing operator g^{xy} . For example, the local weight of the n -gonal face shown in Fig. 3-6 is

$$\begin{aligned} C_{x_1 x_2 \dots x_n} &\equiv C_{a_1 x_1 a_2} g^{a_2 a'_2} C_{a'_2 x_2 a_3} g^{a_3 a'_3} \dots g^{a_n a'_n} C_{a'_n x_n a'_1} g^{a'_1 a_1} \\ &= C_{a_1 x_1}^{a_2} C_{a_2 x_2}^{a_3} \dots C_{a_n x_n}^{a_1} . \end{aligned} \quad (3.1)$$

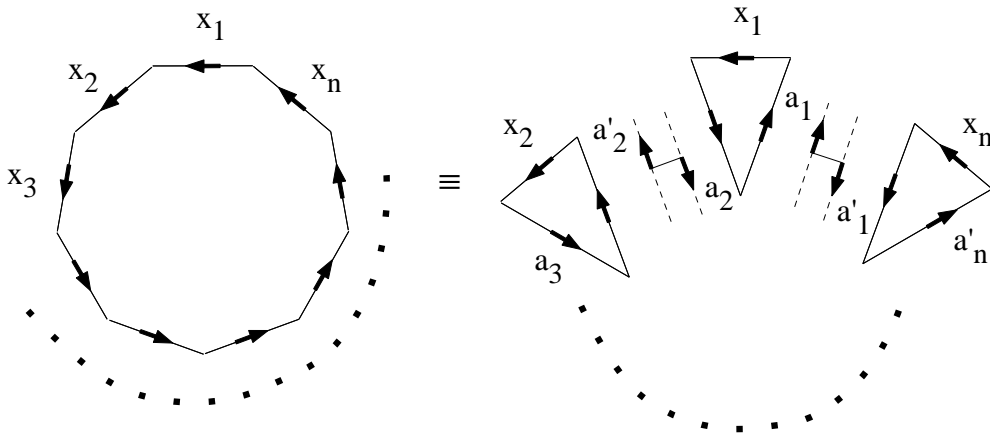


Fig. 3-6: A decomposition of a polygonal face.

For consistency, the definition of polygonal face weights in terms of triangular constituents must be independent of the triangular decomposition chosen. This will be the case if and only if we impose the same two constraints on C_{xyz} and g^{xy} that guaranteed topological invariance of the two–dimensional lattice field theory in sec. 2, namely, invariance under the (2,2) move and the bubble move, eqs. (2.4) and (2.5):

$$\begin{aligned} C_{xy}^u C_{uz}^w &= C_{xu}^w C_{yz}^u \\ C_{xu}^v C_{yv}^u &= g_{xy} , \end{aligned} \quad (3.2)$$

where g_{xy} is the inverse of g^{xy} and will be called the “metric.”

To glue 3–hinges to 3–hinges, we introduce a “hinge–gluing operator” h_{xy} , whose function is to lower the indices of Δ^{xyz} . h_{xy} is represented graphically by a pair of parallel

solid lines with the arrows in the same direction (Fig. 3-7), and always joins hinges with arrows aligned. It is important to remember that just as g^{xy} is used to raise the indices of C_{xyz} only, so h_{xy} can only lower the indices of Δ^{xyz} (and not, *e.g.*, C^{xyz}).

Now we can assign weights to multivalent hinges, with a prescription similar to the prescription for polygonal faces. Namely, just as an n -sided polygon can be decomposed into triangles, an n -valent hinge can be decomposed into a collection of 3-hinges. The weight of an n -hinge is equal to the product of the weights of its constituent 3-hinges, with internal color indices contracted using the hinge-gluing operator h_{xy} . For example, to compute the weight of the 4-hinge Δ^{xyzw} shown in Fig. 3-8a, we can decompose it into two 3-hinges, contracted with a hinge-gluing operator, as in Fig. 3-8b:

$$\Delta^{xyzw} \equiv \Delta^{xyu} h_{uv} \Delta^{vzw} \equiv \Delta^{xyu} \Delta_u{}^{zw} . \quad (3.3)$$

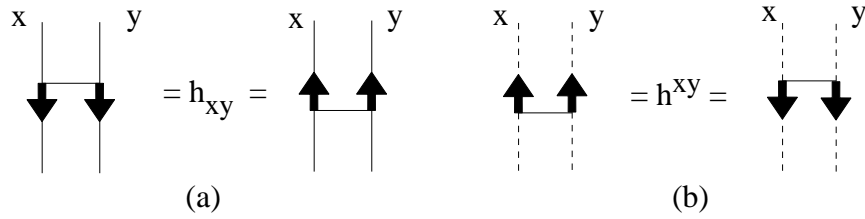


Fig. 3-7: Graphical representation of h_{xy} and h^{xy} .

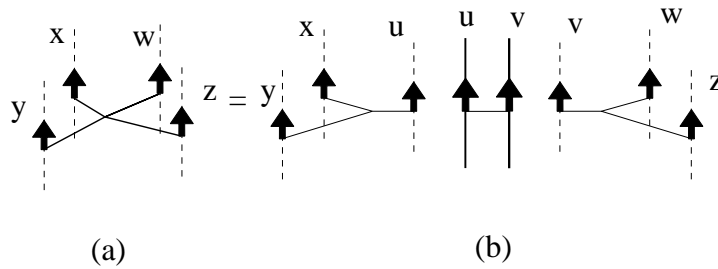


Fig. 3-8: Definition of a 4-hinge.

Similarly, for the n -hinge shown in Fig. 3-9, the corresponding local weight is defined as

$$\Delta^{x_1 x_2 \dots x_n} \equiv \Delta_{a_1}{}^{x_1 a_2} \Delta_{a_2}{}^{x_2 a_3} \dots \Delta_{a_n}{}^{x_n a_1} . \quad (3.4)$$

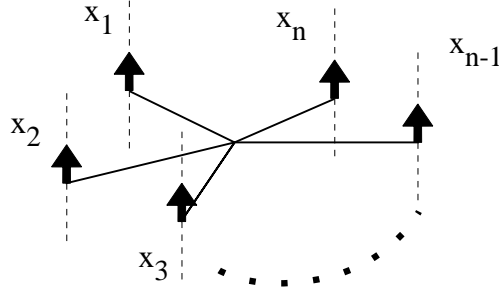


Fig. 3-9: An n -hinge.

As was the case for face weights, consistency requires that our definition of n -hinge weights be independent of the decomposition into 3-hinges chosen. Since, on the plane perpendicular to the n -hinge, this requirement is equivalent to the 2D topological invariance that we imposed on trivalent graphs in subsec. 2.6, we only need to require eqs. (2.30) and (2.31); that is,

$$\Delta_x^{yu} \Delta_u^{zw} = \Delta_x^{uw} \Delta_u^{yz} \quad (3.5)$$

$$\Delta_v^{ux} \Delta_u^{vy} = h^{xy} , \quad (3.6)$$

where h^{xy} is the inverse of h_{xy} and will be called the “cometric.” It may be useful to recall the geometrical meaning of these equations. Eq. (3.5) insures that the definition of Δ^{xyzw} is independent of whether we decompose the 4-hinge as in Fig. 3-10a or b, while eq. (3.6) guarantees that we can collapse a hinge loop, as depicted in Fig. 3-11.

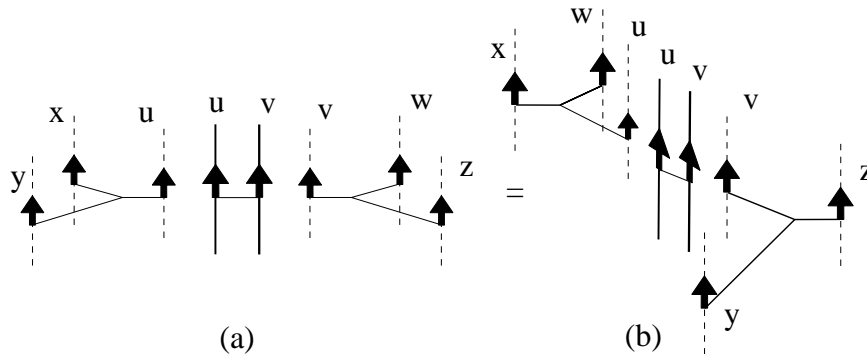


Fig. 3-10: Two different decompositions of a 4-hinge.

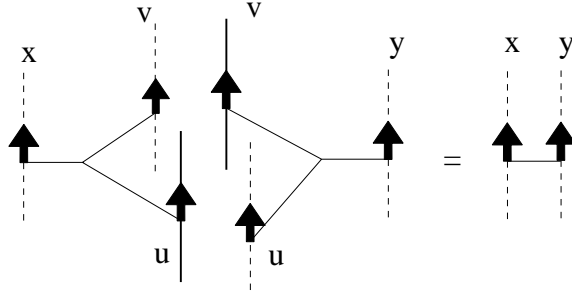


Fig. 3-11: Reduction of a hinge-loop.

Having described how to glue triangles to triangles and 3-hinges to 3-hinges, we still need to explain how to glue triangles to 3-hinges. There are two separate cases to consider, depending on whether the arrows of the face edge and the hinge edge to be joined are in the same direction or in opposite directions.

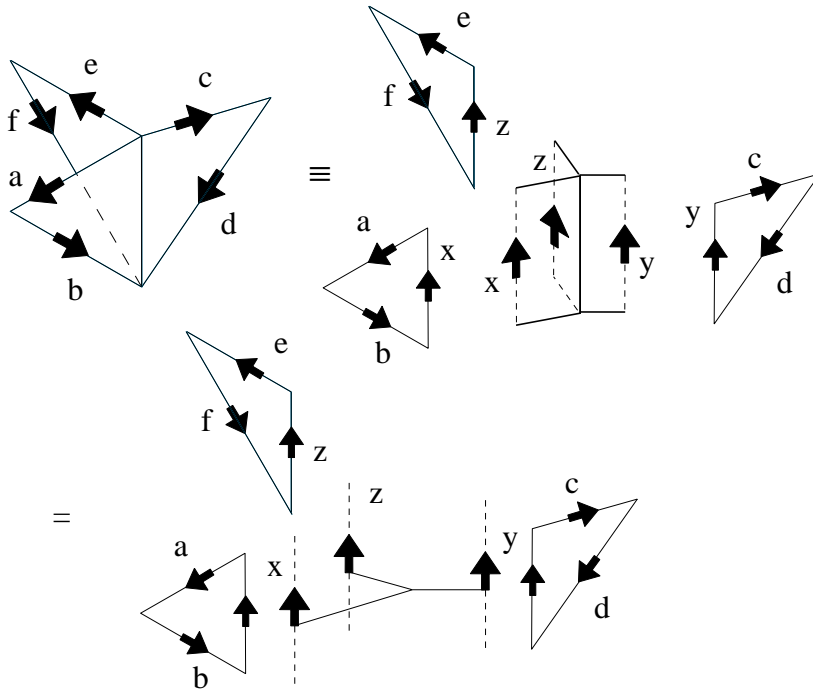


Fig. 3-12: Three triangles joined along a hinge.

For the former case, our gluing rule will be simply to contract the corresponding lower face index and upper hinge index.⁴ For example, the total weight for the configuration of three triangles shown in Fig. 3-12 is $C_{abx}C_{cdy}C_{efz}\Delta^{xyz}$.

⁴ In principle, we could generalize this particular gluing rule by introducing a new gluing oper-

For the latter case, our gluing rule is provided by the operator S_y^x , whose function is to change the direction of an arrow on a hinge. For example, the hinge shown in Fig. 3-13 is assigned the local weight $S_{x'}^x \Delta^{x'yz}$. Because the two hinges in Fig. 3-14 should have the same weight, we require the following constraint between S_y^x and Δ^{xyz} to be satisfied:

$$S_{x'}^x \Delta^{x'yz} = S_{z'}^z S_{y'}^y \Delta^{xz'y'} . \quad (3.7)$$

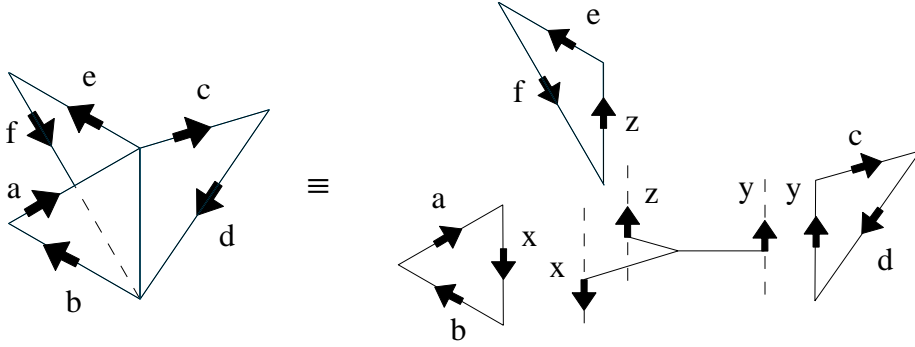


Fig. 3-13: A configuration involving $S_{x'}^x$.

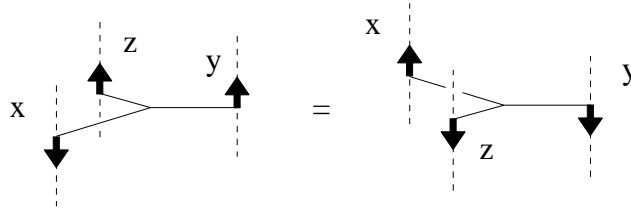


Fig. 3-14: The constraint on S_y^x and Δ^{xyz} .

The five weighting rules we have just described, C_{xyz} , g^{xy} , Δ^{xyz} , h_{xy} , and S_y^x , are the fundamental ingredients in our construction of LFTs. Provided that they satisfy the consistency conditions (3.2), (3.5), (3.6), and (3.7), these data are sufficient to define a

ator Q_y^x , to insert between any 3-hinge and triangle indices to be contracted. However, any such Q_y^x can always be absorbed into the 3-hinge weights by redefining $\widehat{\Delta}^{xyz} \equiv Q_{x'}^x Q_{y'}^y Q_{z'}^z \Delta^{x'y'z'}$; in the new frame $\widehat{Q}_y^x = \delta_y^x$ reduces to our choice of a gluing rule.

lattice field theory; in terms of them, the partition function on an arbitrary lattice L is given by

$$Z(L) = \mathcal{N} \prod_{f: \text{faces}} \prod_{h: \text{hinges}} \prod_{e: \langle x, y \rangle} C_{a_1 a_2 \dots a_k}(f) \Delta^{b_1 b_2 \dots b_l}(h) S^x_y(e), \quad (3.8)$$

where the third product is over pair of glued edges with arrows reversed, all indices are assumed to be contracted, \mathcal{N} is a normalization factor, and $C_{a_1 a_2 \dots a_k}(f)$ and $\Delta^{b_1 b_2 \dots b_l}(h)$ are defined in terms of triangular decompositions of the k -gonal face and the l -hinge, as in eqs. (3.1) and (3.4).

Before closing this subsection, we would like to make two remarks.

The first remark is that our construction of lattice field theories respects lattice duality. To understand this statement more concretely, recall that the dual lattice \tilde{L} of a given lattice L is composed of faces dual to the hinges of L and hinges dual to the faces of L . Thus, given a LFT on the original lattice L with data $(C_{xyz}, g^{xy}, \Delta^{xyz}, h_{xy}, S^x_y)$, we can always define an equivalent lattice theory on the dual lattice \tilde{L} with data $(\tilde{C}_{xyz} \equiv \Delta^{xyz}, \tilde{g}^{xy} \equiv h_{xy}, \tilde{\Delta}^{xyz} \equiv C_{xyz}, \tilde{h}_{xy} \equiv g^{xy}, \tilde{S}^x_y \equiv S^y_x)$. It should be obvious that the partition function of this theory on \tilde{L} is equal to the partition function of the original theory on L .

Finally, we mentioned previously that we could have taken an alternative, more general approach to defining lattice field theories on arbitrary lattices. By allowing the $C_{x_1 x_2 \dots x_k}$ (and the $\Delta^{y_1 y_2 \dots y_l}$) to be independent and not imposing invariance under the subdivision of faces (hinges), we could have defined a much broader class of lattice field theories, with an infinitely larger set of weighting rules, at the expense of an abundance of indices. Our definition of an LFT imposes invariance under face subdivisions at the outset, and thus restricts our discussion to a class of lattice field theories with a limited amount of topological invariance. Alternatively, subdivision invariance could have been imposed at a later stage, along with invariance under other local lattice moves. The end result would have been the same set of TLFTs that we will find later in this section.

3.2. Algebra and Coalgebra Structures in 3D Lattice Field Theories

We will now explain how the data (C_{xyz}, g^{xy}) and (Δ^{xyz}, h_{xy}) can be used to define algebra and coalgebra structures.⁵ As in sec. 2, we introduce a vector space $H \equiv \bigoplus_{x \in X} \mathbf{C} \phi_x$, with one basis element ϕ_x corresponding to each color $x \in X$. Given the data of the LFT

⁵ See Appendix A for definitions of algebra, coalgebra, and related concepts.

defined above, we can define a multiplication operation on H with $C_{xy}^z \equiv C_{xyz'}g^{z'z}$ as structure constants:

$$m : H \otimes H \rightarrow H \quad (3.9)$$

$$m(\phi_x \otimes \phi_y) \equiv \phi_x \cdot \phi_y \equiv C_{xy}^z \phi_z .$$

The consistency requirements (3.2), imposed on any 2D face in our definition of 3D LFTs, imply that the algebra thus defined is associative and semisimple. As explained in subsec. 2.3, such an algebra always contains a unit element u satisfying

$$u : \mathbf{C} \ni 1 \mapsto u(1) = u^x \phi_x \in H$$

$$u(1) \cdot \phi = \phi = \phi \cdot u(1) \quad (3.10)$$

$$i.e. \quad u^x C_{xy}^z = \delta_y^z = u^x C_{yx}^z$$

with $u_x \equiv C_{xa}^a$ and $u^x \equiv g^{xy} u_y$. The last equation is equivalent to the 2D cone equation (2.6), which follows directly from eq. (3.2). For later convenience, we introduce in Fig. 3-15a a graphical representation of u_x as a 2D disc with a color index x on the boundary. Eq. (3.10) (or equivalently eq. (2.6)) is thus depicted in Fig. 3-15b, and is equivalent to the 2D cone move pictured in Fig. 2-3a and b.

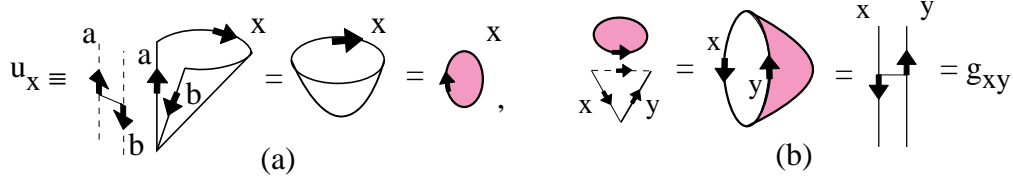


Fig. 3-15: Graphical representation of u_x and (3.10).

Similarly, we can use the hinge weights $\Delta_x^{yz} = h_{xx'}\Delta^{x'yz}$ to define a multiplication operation on the vector space $\tilde{H} \equiv \oplus_{x \in X} \mathbf{C}\tilde{\phi}^x$:

$$\tilde{m} : \tilde{H} \otimes \tilde{H} \rightarrow \tilde{H} \quad (3.11)$$

$$\tilde{m}(\tilde{\phi}^y \otimes \tilde{\phi}^z) \equiv \Delta_x^{yz} \tilde{\phi}^x .$$

It follows from the conditions for invariance under decomposition into 3-hinges, eqs. (3.5) and (3.6), that \tilde{m} is associative and semisimple, and contains a unit element \tilde{u} ,

$$\tilde{u} : \mathbf{C} \ni 1 \mapsto \tilde{u}(1) = \epsilon_x \tilde{\phi}^x \in \tilde{H} \quad (3.12)$$

with $\epsilon_x \equiv h_{xy}\Delta_u^{uy}$.

\tilde{H} is naturally identified with the dual vector space to H , and through this identification, the multiplication \tilde{m} naturally gives rise to a comultiplication operation Δ on H , with the hinge data Δ_x^{yz} as costructure constants:

$$\begin{aligned} \Delta : H &\rightarrow H \otimes H \\ \Delta(\phi_x) &\equiv \Delta_x^{yz} \phi_y \otimes \phi_z . \end{aligned} \tag{3.13}$$

The condition of coassociativity

$$(\Delta \otimes 1_H) \circ \Delta(\phi_w) = (1_H \otimes \Delta) \circ \Delta(\phi_w) \tag{3.14}$$

follows from the associativity of \tilde{m} in \tilde{H} . Furthermore, duality directly implies that the coalgebra (3.13) is ‘‘cosemisimple,’’ and contains a counit ϵ satisfying

$$\begin{aligned} \epsilon : H \ni \phi_x &\mapsto \epsilon(\phi_x) = \epsilon_x \in \mathbf{C} \\ \Delta_x^{yz} \epsilon_z &= \delta_x^y = \epsilon_z \Delta_x^{zy} , \end{aligned} \tag{3.15}$$

with $\epsilon_x \equiv h_{xy} \Delta_u^{xy}$. (See Theorem A.2 in Appendix A for a more detailed discussion of the counit ϵ_x .) In Fig. 3-16a, we introduce a graphical representation for ϵ_x as a single edge with a loop on the plane perpendicular to the edge, and express eq. (3.15), or equivalently, $\epsilon^z \Delta_z^{xy} = h^{xy}$, in Fig. 3-16b.

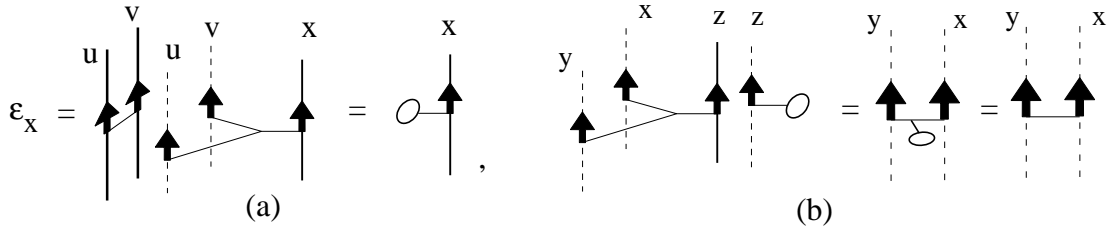


Fig. 3-16: Graphical representation of ϵ_x and (3.15).

A brief remark may serve to clarify the relation between the algebra and the coalgebra structures that we have defined in this subsection. As we have explained, an equivalent lattice theory may be defined on the dual lattice \tilde{L} , whose weights are inherited from the original lattice L . In going to the dual lattice, hinges become faces and faces become hinges, so the structure constants C_{xy}^z and Δ_z^{xy} are simply interchanged, and the algebra and coalgebra respectively determine the coalgebra and the algebra of the dual theory on \tilde{L} .

3.3. Topological Invariance and the Correspondence to Hopf Algebras

In the previous subsection, we showed how to use the data of a three-dimensional lattice field theory (LFT) to define algebra and coalgebra structures on a vector space H . There, the invariance of faces and hinges under subdivision implied that the algebra is associative and semisimple, and the coalgebra is coassociative and cosemisimple. In this subsection, we show that upon requiring our LFT to be topologically invariant, the algebra $(H; m, u)$ and the coalgebra $(H; \Delta, \epsilon)$ are combined to form a constrained Hopf algebra with antipode given by the arrow-reversing operator S appearing in eq. (3.7). (The definition and basic properties of Hopf algebras are discussed in Appendix A.)

To state the main result of this section more precisely, we first introduce an operator T with matrix elements

$$T^x{}_y \equiv h^{xz} g_{zy} , \quad (3.16)$$

and a numerical constant

$$\Lambda_0 \equiv \epsilon_x T^x{}_y u^y = \epsilon^x u_x . \quad (3.17)$$

Then, we will prove the following theorem:

Theorem 3.1. *The set of 3D topological lattice field theories (TLFTs) with data $(C_{xyz}, g^{xy}, \Delta^{xyz}, h_{xy}, S^x{}_y)$ is in one-to-one correspondence with the set of Hopf algebras $(H; m, u, \Delta, \epsilon, S)$ with antipode S of the following form:*

$$S = \frac{1}{\Lambda_0} T . \quad (3.18)$$

An important consequence of eq. (3.18) is that $S^2 = 1$ (see Theorem A.7).⁶

The proof of this theorem is divided into three parts. In Step 1, we will introduce two types of local moves – the hinge move and the 3D cone move – and demand that the partition function $Z(L)$ be invariant under each of them. Invariance under the hinge move will be shown to imply that the quintet $(H; m, u, \Delta, \epsilon)$ forms a bialgebra with a constraint to be given below in eq. (3.21). On the other hand, invariance under the 3D cone move will guarantee that the operator S appearing in eq. (3.7) satisfies the axiom of antipode. Thus, we can conclude that the data $(C_{xyz}, g^{xy}, \Delta^{xyz}, h_{xy}, S^x{}_y)$ of any LFT invariant under the

⁶ This rather restrictive constraint should not be too surprising, since the operation of reversing an arrow twice is trivial. We will discuss the condition $S^2 = 1$ further in sec. 5.

hinge and 3D cone moves defines a Hopf algebra $(H; m, u, \Delta, \epsilon, S)$ with the constraint (3.21), which will be shown in Theorem A.7 to be equivalent to the statement that the antipode S satisfies eq. (3.18). In Step 2, we will prove that these two local moves generate all local, topology-preserving deformations of the lattice. Thus, no additional constraints are needed to guarantee that we have constructed a topologically-invariant LFT, and we can conclude that we have a map from the set of 3D TLFTs to the set of Hopf algebras with antipode $S = \frac{1}{\Lambda_0} T$. In Step 3, we will further show that this map is bijective, *i.e.*, given a Hopf algebra with antipode $S = \frac{1}{\Lambda_0} T$, we can always construct a 3D TLFT. This step will complete the proof of Theorem 3.1.

Step 1.

Our starting point is a simple identity, the “hinge equation,” which expresses algebraically a necessary condition for topological invariance. It is derived from a topology-preserving move that takes two triangles glued to each other along two hinges, and collapses them homotopically to a single triangle plus a hinge (and vice versa). Picture the triangles as forming a conical tube, as in Fig. 3-17, possibly with additional faces attached to the two hinges. Then provided that none of these additional faces are attached to the hinges in the *interior* of the tube, we can squeeze it from the bottom and flatten it as we go up, like a tube of toothpaste, pushing out any structure attached to the two open edges (labeled a and b in Fig. 3-17) and ending up with a single flat triangle attached to a hinge. We call this operation the “hinge move,” and call the equation expressing the invariance under the hinge move the hinge equation. (A similar move, which collapses two triangles glued together along all three edges to a single triangle, is derived from the hinge move in Appendix B.) The hinge equation is reminiscent of the two-dimensional bubble equation (2.5), which told us how to collapse two triangles sharing two edges to a single edge. (See Fig. 2-2.)

The expression of invariance under the hinge move in terms of the local weights can be deduced from a careful inspection of Fig. 3-17 as follows:

$$\Delta_x^{pq} \Delta_y^{rs} C_{apr} C_{bqs} = \Lambda C_{xyz} \Delta^z_{ba} . \quad (3.19)$$

Here, a numerical factor Λ is introduced to count the number of 3D cells, and will be determined below.

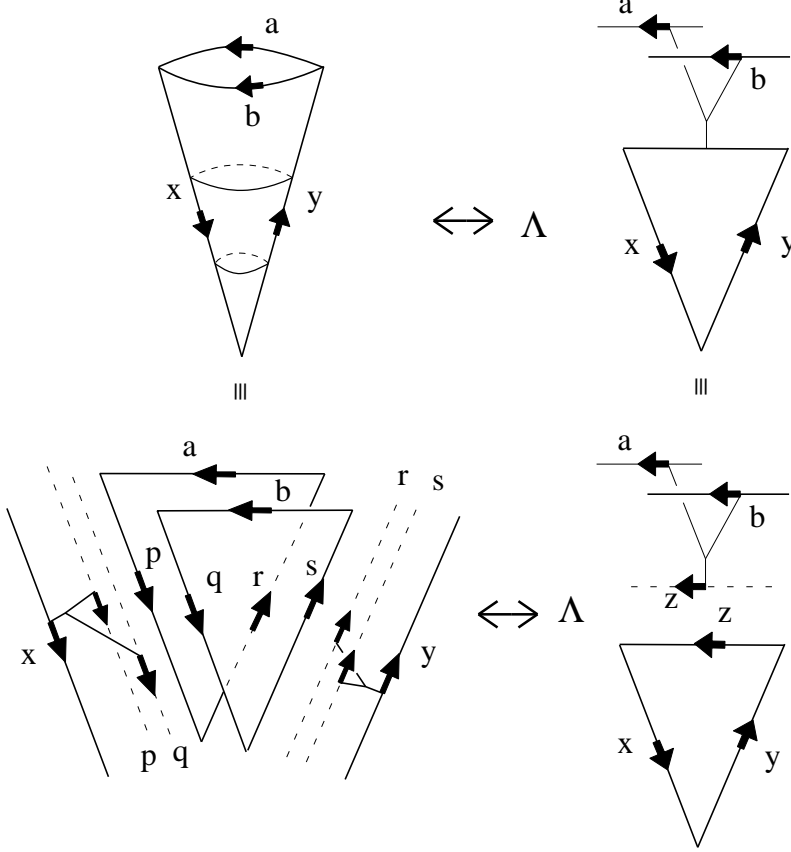


Fig. 3-17: The hinge move.

To obtain an algebraic interpretation of eq. (3.19), we first need the following identities, whose proofs are contained in Appendix B:

$$\begin{aligned}
 u^x \Delta_x^{yz} &= u^y u^z \\
 C_{xy}{}^z \epsilon_z &= \epsilon_x \epsilon_y .
 \end{aligned}
 \tag{3.20}$$

Multiplying both sides of eq. (3.19) by u^x and using (3.20), we find

$$T_r^a T_s^b \Delta_y^{rs} = \Lambda T_y^z \Delta_z^{ba} ,
 \tag{3.21}$$

where we have used $T_r^a = h^{aa'} g_{a'r}$. Note that eq. (3.21) is equivalent to the statement that $\frac{1}{\Lambda} T$ is a coalgebra antimorphism [29]. Next we substitute eq. (3.21) into eq. (3.19), and obtain

$$\Delta_x^{pq} \Delta_y^{rs} C_{pr}{}^a C_{qs}{}^b = C_{xy}{}^z \Delta_z^{ab} .
 \tag{3.22}$$

This equation is equivalent to the statement that comultiplication Δ is an algebra morphism with respect to multiplication m , $\Delta(\phi_x \cdot \phi_y) = \Delta(\phi_x) \cdot \Delta(\phi_y)$. More precisely,

$$\Delta \circ m(\phi_x \otimes \phi_y) = (m \otimes m) \circ (1 \otimes \tau \otimes 1) \circ (\Delta \otimes \Delta)(\phi_x \otimes \phi_y), \quad (3.23)$$

where τ is the twist mapping:

$$\tau : H \otimes H \ni \phi_a \otimes \phi_b \mapsto \phi_b \otimes \phi_a \in H \otimes H. \quad (3.24)$$

Furthermore, multiplying eq. (3.22) by $u^y \epsilon_b$, and using eqs. (3.10), (3.15) and (3.20), we obtain $\delta_x^a = \delta_x^a u^y \epsilon_y$, or

$$\epsilon_x u^x = 1. \quad (3.25)$$

Remarkably, eqs. (3.20), (3.22) and (3.25) are exactly the conditions for $(H; m, u, \Delta, \epsilon)$ to be a bialgebra (see Appendix A). That is,

Lemma 3.2. *The hinge equation (3.19) and eq. (3.20) imply that the quintet $(H; m, u, \Delta, \epsilon)$ forms a bialgebra with the constraint (3.21).*

Next, we will show that the lattice operator S defined in subsec. 3.1 is the antipode of a Hopf algebra $(H; m, u, \Delta, \epsilon, S)$, by considering a configuration in which two edges of a single triangle are glued together on a hinge, and imposing invariance under a particular local move that removes such a triangle. Because a triangle of this sort looks like a cone, we will refer to this move as the “3D cone move.” Its effect is to contract the surface of the cone down to a minimal-area surface bounded by the edges of the original triangle; the result looks like a vertical edge, labeled x in Fig. 3-18, attached at the bottom to a disc with boundary y .

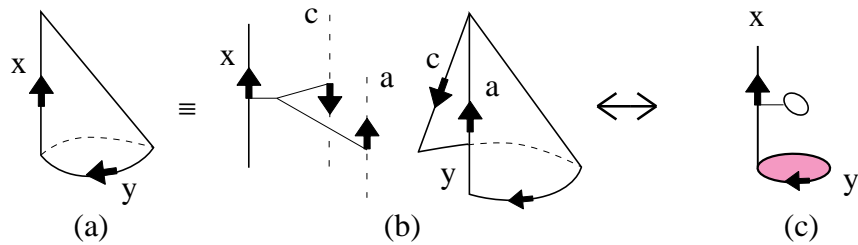


Fig. 3-18: 3D cone move.

Invariance under the particular cone move shown in Fig. 3-18 implies that

$$\Delta_x^{ab} S_b^c C_{ac}^y = u^y \epsilon_x . \quad (3.26)$$

By changing the orientations of the edges x and y , and imposing invariance under three nearly identical cone moves, we obtain the following set of identities:

$$\Delta_x^{ab} S_a^c C_{cb}^y = u^y \epsilon_x \quad (3.27)$$

$$\Delta_x^{ab} S_b^c C_{ca}^y = u^y \epsilon_x \quad (3.28)$$

$$\Delta_x^{ab} S_a^c C_{bc}^y = u^y \epsilon_x . \quad (3.29)$$

Eqs. (3.26) and (3.27) are the defining axioms for antipode S of a Hopf algebra, and (3.28) and (3.29) are equivalent to the property $S^2 = 1$ (see Appendix A):

$$\begin{aligned} m \circ (S \otimes 1) \circ \Delta &= m \circ (1 \otimes S) \circ \Delta = u \circ \epsilon \\ S^2 &= 1 . \end{aligned} \quad (3.30)$$

Furthermore, due to Theorem A.7, the constraint (3.21) on T implies that $\Lambda = \Lambda_0$, and the antipode S has the following form:

$$S = \frac{1}{\Lambda_0} T , \quad (3.31)$$

from which we can again conclude that $S^2 = 1$. Thus, we have proven

Lemma 3.3. *Invariance under the hinge move, 3D cone moves, and Eq. (3.20) imply that the sextet $(H; m, u, \Delta, \epsilon, S)$ forms a Hopf algebra with antipode $S = \frac{1}{\Lambda_0} T$.*

Note that the consistency condition (3.7) is automatically satisfied since

$$\begin{aligned} S_b^y S_c^z \Delta^{xcb} &= S_b^y S_c^z h^{xx'} \Delta_{x'}^{cb} = h^{xx'} S_{x'}^{a'} \Delta_{a'}^{yz} \\ &= h^{xx'} S_{x'}^{a'} h_{a'a} \Delta^{ayz} = \frac{1}{\Lambda_0} h^{xx'} h^{a'b} g_{bx'} h_{a'a} \Delta^{ayz} \\ &= S_a^x \Delta^{ayz} . \end{aligned} \quad (3.32)$$

by eqs. (3.16), (3.21), and (3.31).

Step 2.

The hinge and 3D cone moves are simple yet powerful moves relating topologically equivalent lattices. Another move we have discussed is the subdivision of a polygonal face

into two or more polygons. We claim that these moves are sufficient to generate all lattices in a given topological equivalence class. The method of our proof will be to show that these moves generate a set of standard moves, which are sufficient by Alexander’s theorem.

Theorem 3.4. *Any local deformation of a 3D lattice can be generated by a sequence of hinge, 3D cone, and face–subdivision moves.*

Proof. Given two topologically equivalent lattices L and L' , we must show the existence of an interpolating sequence of topology–preserving deformations. We begin by triangulating all polygonal faces in L and L' , and using hinge and 3D cone moves to eliminate any pairs of triangles with two edges in common as well as any single triangles with two edges meeting at a hinge. The resulting “good” triangulations \bar{L} and \bar{L}' have the property that at least three triangles will always meet at any vertex of any polyhedron. We would then like to show that hinge moves and face–subdivision moves are sufficient to decompose each resulting polyhedron into tetrahedra. Let us postpone the proof of this statement for the moment, and see how the theorem follows once a tetrahedral decomposition has been constructed.

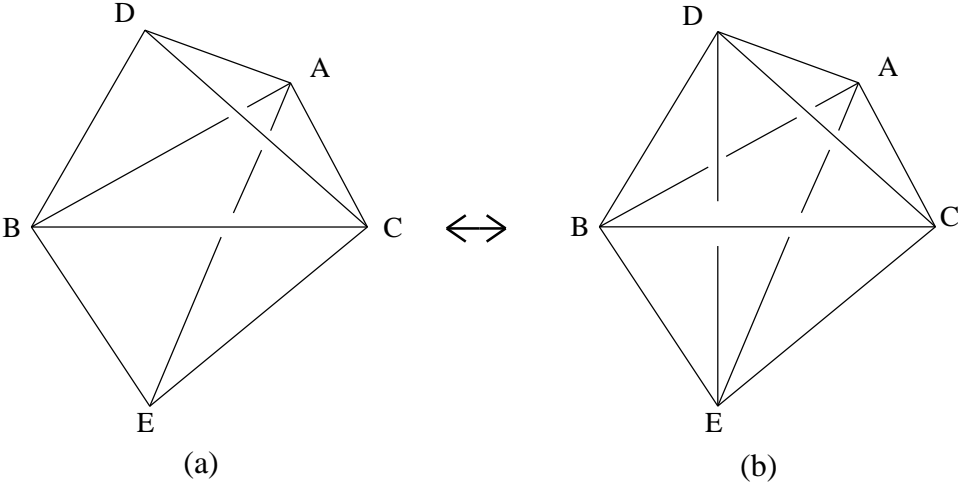


Fig. 3-19: (2,3) move.

Then \bar{L} and \bar{L}' can be respectively decomposed into two topologically equivalent tetrahedral lattices Γ and Γ' . At this point, we invoke a version [13][14] of Alexander’s theorem [26], according to which any two topologically equivalent tetrahedral lattices are related by a sequence of special local lattice moves, known as “(2,3)” and “bubble” moves (Fig. 3-19 and Fig. 3-20). The (2,3) move relates a configuration containing two

tetrahedra joined along a face to a configuration in which the two tetrahedra have been replaced by three tetrahedra joined along a hinge (which is dual to the original face), while the bubble move collapses two tetrahedra sharing three faces to a single triangle. Both types of moves are explained in detail in Appendix B, and shown to be generated by sequences of hinge and face-subdivision moves. Thus, the sequence of (2,3) and bubble moves interpolating between Γ and Γ' can be reduced to a sequence of hinge moves, which can in turn be incorporated into a sequence of hinge, 3D cone, and face-subdivision moves interpolating between L and L' .

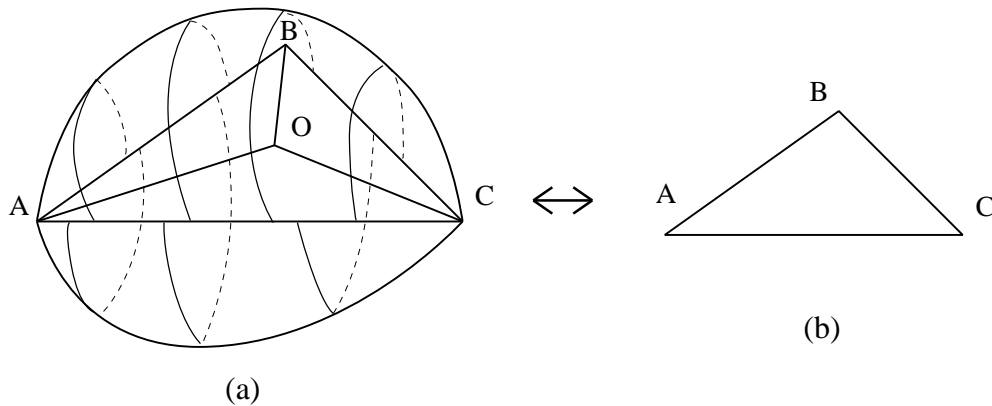


Fig. 3-20: 3D Bubble move

It remains to prove our assertion that hinge and face-subdivision moves alone are sufficient to decompose a triangulated polyhedron into tetrahedra. We will perform an induction on the number of faces F of the polyhedron P . Recall that our “good” triangulation has been chosen so that at least three triangles always meet at any vertex of P . Let us choose a vertex O at which m triangles meet (Fig. 3-21).

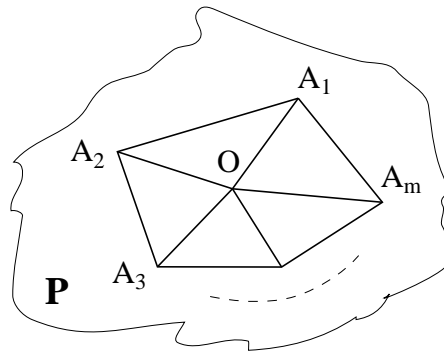


Fig. 3-21: m triangles meeting at a vertex O .

In order to visualize three-dimensional lattice operations more clearly, we raise the position of the vertex O as shown in Fig. 3-22a, relative to Fig. 3-21. Now consider the two adjacent triangles OA_1A_2 and OA_2A_3 , singled out in Fig. 3-23. By applying the hinge move to these triangles twice, we obtain two additional internal triangles with the same vertices, joined by a face-gluing operator. (This process of “inflation” is described in detail in Lemma B.4.) After acting on these internal triangles with a (2,2) move, the resulting internal triangles OA_1A_3 and $A_1A_2A_3$ together with the two external triangles OA_1A_2 and OA_2A_3 make up the four faces of a tetrahedron. We now repeat this process of tetrahedron-formation on the successive pairs of adjacent triangles OA_1A_k and OA_kA_{k+1} ($k = 3, \dots, m - 1$), obtaining finally $m - 2$ interior tetrahedra shown in Fig. 3-22b, whose external faces are the original m triangles that we started with.⁷ After removing these tetrahedra in Fig. 3-22c, we are left with a polyhedron with $F - 2$ faces (also obeying the “good” condition), to which the induction hypothesis can be applied.

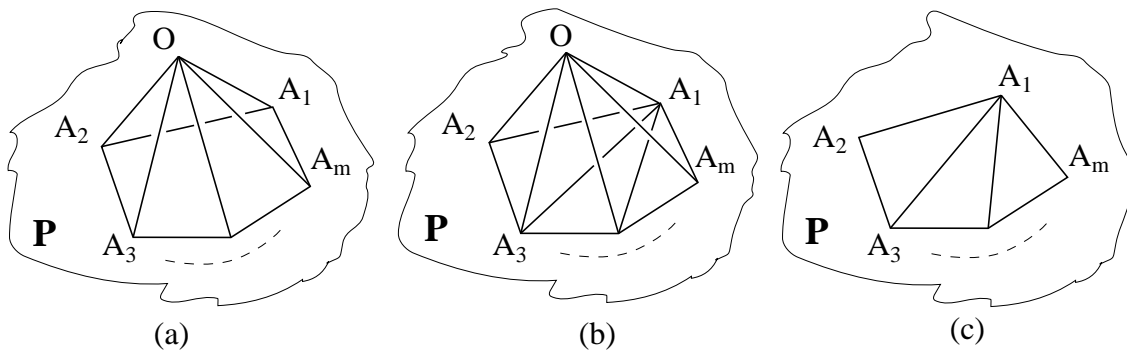


Fig. 3-22: Inductive construction of a tetrahedral decomposition.

We continue reducing the number of faces until we eventually reach a good polyhedron with four faces, that is, a tetrahedron. (Here we make use of the fact that our polyhedral 3-cells are all contractible.) At this point, the construction of a tetrahedral decomposition of P is complete, and so is the proof. (QED)

Step 3.

⁷ More precisely, the resulting configuration includes an inflated triangular tube OA_mA_1 , which can be flattened by a hinge move, as described in Lemma B.2.

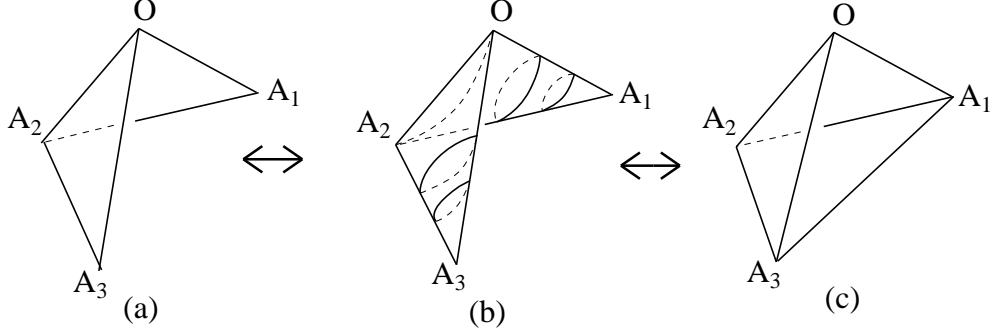


Fig. 3-23: Construction of a tetrahedron using hinge moves.

The preceding lemma implies the existence of a map from the set of 3D TLFTs to the set of Hopf algebras with antipode $S = \frac{1}{\Lambda_0} T$. In this step, we further prove that this map is bijective. Given a Hopf algebra $(H; m, u, \Delta, \epsilon, S)$ with antipode $S = \frac{1}{\Lambda_0} T$, we first define the metric and the cometric by

$$\begin{aligned} g_{xy} &= C_{xa}{}^b C_{yb}{}^a \\ h^{xy} &= \Delta_a{}^{bx} \Delta_b{}^{ay} , \end{aligned} \tag{3.33}$$

which can be used to define the cyclic local weights $C_{xyz} \equiv g_{zz'} C_{xy}{}^{z'}$ and $\Delta^{xyz} \equiv h^{xx'} \Delta_{x'}{}^{yz}$. Since S is a coalgebra antimorphism, we can show that S_r^q satisfies eq. (3.7), using the same sequence of manipulations that appeared in eq. (3.32). In other words, we can consistently assign a local weight to a hinge whose arrows are not in the same direction. A 3D LFT can thus be constructed from the data $(C_{xyz}, g^{xy}, h_{xy}, \Delta^{xyz}, S_r^q)$. Moreover, the Hopf algebra axioms and the form of the antipode will ensure that this 3D LFT satisfies the hinge equation (3.19) and the cone identities (3.26)–(3.29). Thus, given a Hopf algebra with $S = \frac{1}{\Lambda_0} T$, we can always construct a 3D TLFT.

4. Example: $H = \mathbf{C}[G]$ and the Ponzano–Regge Models

We now apply the results of the preceding section to the group ring $H = \mathbf{C}[G]$ of a compact group:

$$H = \mathbf{C}[G] = \bigoplus_{x \in G} \mathbf{C} \phi_x . \tag{4.1}$$

Although $\mathbf{C}[G]$ is one of the simplest examples of a Hopf algebra, it contains enough structure to provide a good illustration of the concepts of Section 3, and to lead to an interesting topological lattice field theory.

In subsec. 4.1, we review the Hopf algebra structure of $\mathbf{C}[G]$. Next, in subsec. 4.2, we construct the TLFT associated with $H = \mathbf{C}[G]$ and relate it to a lattice gauge theory with heat–kernel action. Finally, in subsec. 4.3, we will further relate this TLFT to the lattice theory of Ponzano and Regge [17,14].

4.1. $H = \mathbf{C}[G]$ as a Hopf algebra

Let G be a compact group. $H = \mathbf{C}[G]$ becomes a Hopf algebra if we define (bi-)linear maps m , u , Δ , ε and S as follows:

(i) multiplication

$$m : H \otimes H \ni \phi_x \otimes \phi_y \mapsto \phi_{xy} \in H \quad (4.2)$$

(ii) unit

$$u : \mathbf{C} \ni 1 \mapsto \phi_{1_G} \in H \quad (4.3)$$

(iii) comultiplication

$$\Delta : H \ni \phi_x \mapsto \phi_x \otimes \phi_x \in H \otimes H \quad (4.4)$$

(iv) counit

$$\varepsilon : H \ni \phi_x \mapsto 1 \in \mathbf{C} \quad (4.5)$$

(v) antipode

$$S : H \ni \phi_x \mapsto \phi_{x^{-1}} \in H . \quad (4.6)$$

It is easy to show that these definitions satisfy the Hopf algebra axioms, which are given in Appendix A. This Hopf algebra is cocommutative, and has an antipode S obeying $S^2 = 1$.

Eqs. (4.2) - (4.5) determine the structure constants C_{xy}^z and the costructure constants Δ_x^{yz} as

$$\begin{aligned} C_{xy}^z &= \delta(xy, z) \\ \Delta_x^{yz} &= \delta(x, y) \delta(x, z) . \end{aligned} \quad (4.7)$$

The metric and cometric are obtained by combining eq. (4.7) with eqs. (3.2), (3.6), (3.10) and (3.15):

$$\begin{aligned} g_{xy} &= \delta(x, y^{-1}) & g^{xy} &= \delta(x, y^{-1}) \\ u^x &= \delta(x, 1_G) & u_x &= \delta(x, 1_G) \\ h^{xy} &= |G| \delta(x, y) & h_{xy} &= \frac{1}{|G|} \delta(x, y) \\ \epsilon_x &= 1 & \epsilon^x &= |G| \end{aligned} \quad (4.8)$$

with $|G| \equiv \text{card}(G) = \delta(x, x)$.⁸ The numerical constant Λ_0 appearing in eq. (3.17) is determined as

$$\Lambda_0 = \int dx \epsilon^x u_x = |G| . \quad (4.9)$$

It is easy to see that the condition (3.18) is satisfied for this Hopf algebra:

$$\frac{1}{\Lambda_0} T^x_y = \frac{1}{\Lambda_0} \int dz h^{xz} g_{zy} = \delta(x, y^{-1}) = S^x_y . \quad (4.10)$$

Thus, due to Theorem 3.1, we can construct a TLFT with the following data $(C_{xyz}, g^{xy}, \Delta^{xyz}, h_{xy}, S^x_y)$:

$$\begin{aligned} C_{xyz} &\equiv \int dz' C_{xy}{}^{z'} g_{z'z} = \delta(xyz, 1_G) \\ g^{xy} &= \delta(x, y^{-1}) \\ \Delta^{xyz} &\equiv \int dx' h^{xx'} \Delta_{x'}{}^{yz} = |G| \delta(x, y) \delta(x, z). \\ h_{xy} &= \frac{1}{|G|} \delta(x, y) \\ S^x_y &= \delta(x, y^{-1}) . \end{aligned} \quad (4.11)$$

The contribution from an arbitrary polygonal face can be evaluated as in eq. (3.1):

$$\begin{aligned} C_{x_1 x_2 \dots x_n} &= \int da_1 da_2 \dots da_n da'_1 da'_2 \dots da'_n g^{a_1 a'_1} \dots g^{a_n a'_n} \\ &\quad \times C_{a_1 x_1 a_2} C_{a'_2 x_2 a_3} \dots C_{a'_n x_n a'_1} \\ &= \delta(x_1 x_2 \dots x_n, 1_G) . \end{aligned} \quad (4.12)$$

Hence, in configurations with nonzero weight, the product of the link variables around each two-dimensional cell is constrained to equal the unit element of G .

On the other hand, the contribution of a hinge joining n faces, as given by the generalized hinge operator of eq. (3.5), is easily seen to be

$$\Delta^{x_1 x_2 \dots x_n} = |G| \delta(x_1, x_2) \delta(x_1, x_3) \dots \delta(x_1, x_n) . \quad (4.13)$$

Eq. (4.13) implies that the edges which are connected to the same hinge have the same value in G .

⁸ Since $|G|$ is infinite in a continuous group, the following discussion is of a somewhat formal nature.

Using these expressions for $C_{x_1 x_2 \dots x_n}$ and $\Delta^{x_1 x_2 \dots x_n}$ we can now write down the partition function $Z(L)$ for a given cellular decomposition L as⁹

$$Z(L) = \frac{1}{|G|^{N_3(L)}} \int \prod_{l \in C_1} dx_l \prod_{f \in C_2} \delta \left(\prod_{l \in f} x_l, 1_G \right). \quad (4.14)$$

Here, C_r denotes the set of r -dimensional cells, and $N_r(L)$ is the number of r -dimensional cells; $N_r(L) \equiv |C_r|$. As was explained in sec. 3, the direction of each link variable x_l ($l \in C_1$) should be fixed before its integration, although the final answer is independent of the direction.

4.2. Relation to topological lattice gauge theory

The framework and results of the previous subsection are strongly reminiscent of lattice gauge theory (LGT), where one also associates a group element to each link of the lattice. In fact, the TLFT based on $H = \mathbf{C}[G]$ reproduces the zero coupling limit of LGT [14] in the following way.

First, we define the partition function of the heat-kernel LGT action for a cellular decomposition L , at inverse temperature β (related to the bare coupling g_0 as $\beta \sim 1/g_0^2$), to be [30]

$$\begin{aligned} Z_\beta^{\text{LGT}}(L) &\propto \int \prod_{l \in C_1} dx_l \prod_{f \in C_2} e^{-S_\beta(U_f)} \\ e^{-S_\beta(U_f)} &\equiv \sum_j d_j \chi_j(U_f) e^{-Q_j/\beta}. \end{aligned} \quad (4.15)$$

Here, U_f is a plaquette variable for a face $f \in C_2$ ($U_f \equiv \prod_{l \in f} x_l$), and d_j , χ_j and Q_j are the dimension, the character and the quadratic Casimir of an irreducible representation j , respectively. Now taking the zero coupling limit $\beta \rightarrow \infty$ ($g_0 \rightarrow 0$) in eq. (4.15), we find

$$e^{-S_\beta(U_f)} \xrightarrow{\beta \rightarrow \infty} \sum_j d_j \chi_j(U_f) = \delta(U_f, 1_G) = \delta \left(\prod_{l \in f} x_l, 1_G \right), \quad (4.16)$$

and thus $\lim_{\beta \rightarrow \infty} Z_\beta^{\text{LGT}}(L)$ actually yields the same expression as eq. (4.14) up to an irrelevant normalization factor.

⁹ The normalization factor \mathcal{N} can be calculated as $|G|^{-N_3(L)}$ from the factors of $\Lambda = |G|$ appearing in the (2,3) and bubble moves, as described in Appendix B.

The topological nature of the zero coupling limit of LGT has a simple explanation in the continuum limit. As $g_0 \rightarrow 0$, the kinetic term

$$\frac{1}{g_0^2} \int d^3x \operatorname{Tr} F_{\mu\nu} F^{\mu\nu} \quad (4.17)$$

becomes peaked about flat connections with $F_{\mu\nu} \equiv 0$, for which the action vanishes. The path integral then collapses to an integral over gauge-inequivalent flat connections. Likewise, in the TLFT for $\mathbf{C}[G]$, the form of the generalized structure constants $C_{x_1 \dots x_k} = \delta(x_1 x_2 \dots x_k, 1_G)$ imposes a lattice analogue of the flatness constraint on those configurations that contribute with nonzero weight. Thus, in the continuum limit, the partition function (4.14) also becomes an integral over flat connections.

4.3. Relation to the Ponzano–Regge Model

In this subsection, we show that the partition function of the TLFT associated with $H = \mathbf{C}[G]$ for $G = \mathrm{SU}(2)$ reproduces that of Ponzano and Regge [17], which is equal to the classical ($q=1$) Turaev–Viro invariant [18]. Our derivation follows the logic of ref. [14].

The Ponzano–Regge model is defined as follows. We first take a tetrahedral cell decomposition L and color the links with representations of $\mathrm{SU}(2)$. To each tetrahedron, we then assign a numerical weight, the $6j$ -symbol of $\mathrm{SU}(2)$ corresponding to the representations on the six edges of the tetrahedron. The partition function is then (essentially) the sum over colorings of the product of the tetrahedral weights,

$$Z_{\mathrm{PR}}(L) \equiv \frac{1}{|G|^{N_0(L)}} \sum_{\{j\}} \left(\prod_{l \in C_1} d_{j_l} \right) \prod_{T \in C_3} \left\{ \begin{matrix} j_{T_1} & j_{T_2} & j_{T_3} \\ j_{T_4} & j_{T_5} & j_{T_6} \end{matrix} \right\}. \quad (4.18)$$

(The notation of this expression will be explained below.)

We will show that the partition function (4.18) of the tetrahedral complex L is equal to the partition function of the TLFT defined on the same lattice for the dual Hopf algebra $\widetilde{H} = \widetilde{\mathbf{C}[G]}$ (see the remark after Corollary A.6). The dual Hopf algebra $\widetilde{H} = \widetilde{\mathbf{C}[G]}$ has the following structure constants:

$$\begin{aligned} \widetilde{C}_{xy}{}^z &= \delta(x, z) \delta(y, z) \\ \widetilde{\Delta}_x{}^{yz} &= \delta(x, yz) \end{aligned} \quad (4.19)$$

as is easily read out from eq. (4.7). The lattice theory is thus defined by the following data:

$$\begin{aligned}
\tilde{C}_{xyz} &= |G| \delta(x, y) \delta(x, z) & \tilde{\Delta}^{xyz} &= \delta(xyz, 1_G) \\
\tilde{g}^{xy} &= \frac{1}{|G|} \delta(x, y) & \tilde{h}_{xy} &= \delta(xy, 1_G) \\
\tilde{u}^x &= 1 & \tilde{\epsilon}_x &= \delta(x, 1_G) .
\end{aligned} \tag{4.20}$$

For the generalized weights we have

$$\begin{aligned}
\tilde{C}_{x_1 x_2 \dots x_n} &= |G| \delta(x_1, x_2) \cdots \delta(x_1, x_n) \\
\tilde{\Delta}^{x_1 x_2 \dots x_n} &= \delta(x_1 x_2 \cdots x_n, 1_G) .
\end{aligned} \tag{4.21}$$

Due to the delta functions, the only configurations that contribute with nonzero weight are those in which every link around every face is mapped to the same group element, and in which the product of the group elements on all the edges joined at any hinge is equal to 1_G . Therefore, the partition function of this TLFT is equal to¹⁰

$$Z(L) = \frac{1}{|G|^{N_0(L)}} \int \prod_{f \in C_2} dx_f \prod_{h \in C_1} \delta \left(\prod_{f \text{ around } h} x_f, 1_G \right) , \tag{4.22}$$

where x_f are the face variables around the hinge h .

To evaluate this partition function (4.22), we first rewrite the delta function on the hinge h in terms of the matrix elements of $x \in G$ in an irreducible representation j_h :

$$D_{mn}^{j_h}(x) \equiv \langle j_h, m | x | j_h, n \rangle , \tag{4.23}$$

where m and n are weight vectors in the representation j_h . Recall here that they satisfy the following equations [31]:

$$\begin{aligned}
\int dx D_{mn}^j(x) D_{m'n'}^{j'}(x^{-1}) &= \frac{1}{d_j} \delta^{jj'} \delta_{mm'} \delta_{nn'} \\
\sum_m D_{lm}^j(x) D_{mn}^j(y) &= D_{ln}^j(xy) \\
\sum_m D_{mm}^j(x) &= \chi_j(x) .
\end{aligned} \tag{4.24}$$

¹⁰ The normalization factor $|G|^{-N_0(L)}$ can be obtained from the normalization factor in eq. (4.14) by a duality transformation.

Thus, by using eq. (4.24) we can re-express the δ -function in eq. (4.22) as a product of matrix elements:

$$\begin{aligned} \delta \left(\prod_{f \text{ around } h} x_f, 1_G \right) &= \sum_{j_h} d_{j_h} \chi_{j_h}(x_1 x_2 \dots x_n) \\ &= \sum_{j_h, \{m_i\}} d_{j_h} D_{m_1 m_2}^{j_h}(x_1) D_{m_2 m_3}^{j_h}(x_2) \dots D_{m_k m_1}^{j_h}(x_n) . \end{aligned} \quad (4.25)$$

Substituting this expression back to eq. (4.22), the partition function becomes

$$Z(L) = \frac{1}{|G|^{N_0(L)}} \int \prod_{f \in C_2} dx_f \prod_{h \in C_1} \sum_{j_h, \{m_i\}} d_{j_h} D_{m_1 m_2}^{j_h}(x_1) D_{m_2 m_3}^{j_h}(x_2) \dots D_{m_k m_1}^{j_h}(x_n) . \quad (4.26)$$

Now since all faces are triangular, each x_f appears three times in the product over hinges. So we can rewrite the product as a product over faces:

$$\begin{aligned} Z(L) &= \frac{1}{|G|^{N_0(L)}} \sum_{\{j\}} \left(\prod_{h \in C_1} d_{j_h} \right) \\ &\quad \sum_{\{m_{f_i}, n_{f_i}\}} \int \prod_{f \in C_2} dx_f D_{m_{f_1} n_{f_1}}^{j_{f_1}}(x_f) D_{m_{f_2} n_{f_2}}^{j_{f_2}}(x_f) D_{m_{f_3} n_{f_3}}^{j_{f_3}}(x_f) , \end{aligned} \quad (4.27)$$

where the indices $\{m_{f_i}, n_{f_i}\}$ (for $i = 1, 2, 3$) should be contracted in such a way that they form a trace around each hinge h as is shown in eq. (4.25). In eq. (4.27), we notice that for each face variable, x_f , there are three representations j_{f_i} , for $i = 1, 2, 3$, associated with the three edges.

In the following, we restrict ourselves to the case $G = SU(2)$; $m = -j, -j+1, \dots, j-1, j$ and $d_j = 2j+1$. In this case, we have the additional equations [31]

$$\int dx D_{m_1 n_1}^{j_1}(x) D_{m_2 n_2}^{j_2}(x) D_{m_3 n_3}^{j_3}(x) = \begin{pmatrix} j_1 & j_2 & j_3 \\ m_1 & m_2 & m_3 \end{pmatrix} \begin{pmatrix} j_1 & j_2 & j_3 \\ n_1 & n_2 & n_3 \end{pmatrix} \quad (4.28)$$

and

$$D_{mn}^j(x^{-1}) = (-1)^{(j+m)+(j+n)} D_{-n-m}^j(x) . \quad (4.29)$$

Here, $\begin{pmatrix} j_1 & j_2 & j_3 \\ m_1 & m_2 & m_3 \end{pmatrix}$ is Wigner's $3j$ -symbol

$$\begin{pmatrix} j_1 & j_2 & j_3 \\ m_1 & m_2 & m_3 \end{pmatrix} = \frac{(-1)^{j_1-j_2-m_3}}{\sqrt{d_j}} \langle j_1 j_2, m_1 m_2 | j_3, -m_3 \rangle , \quad (4.30)$$

and eq. (4.29) expresses the G -parity invariance of $SU(2)$. Thus by integrating over x_f , we obtain two $3j$ -symbols for each face f . The product over faces of $3j$ -symbols can be rearranged into a product over tetrahedra of $6j$ -symbols

$$\left\{ \begin{matrix} j_1 & j_2 & j_3 \\ j_4 & j_5 & j_6 \end{matrix} \right\} \equiv \sum_{\{m_i\}} (-1)^{j_4+j_5+j_6+m_4+m_5+m_6} \cdot \left(\begin{matrix} j_1 & j_2 & j_3 \\ m_1 & m_2 & m_3 \end{matrix} \right) \left(\begin{matrix} j_5 & j_6 & j_1 \\ m_5 & -m_6 & m_1 \end{matrix} \right) \left(\begin{matrix} j_6 & j_4 & j_2 \\ m_6 & -m_4 & m_2 \end{matrix} \right) \left(\begin{matrix} j_4 & j_5 & j_3 \\ m_4 & -m_5 & m_3 \end{matrix} \right). \quad (4.31)$$

The four faces whose $3j$ -symbols appear here form a tetrahedron, as shown in Fig. 4-1.

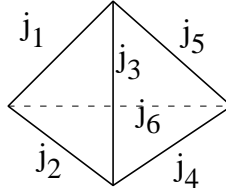


Fig. 4-1: A tetrahedron with edge variables j_i .

Performing the integration in eq. (4.27) and using eqs. (4.28) and (4.29), we finally obtain the partition function on L [14]

$$Z(L) = \frac{1}{|G|^{N_0(L)}} \sum_{\{j\}} \left(\prod_{h \in C_1} d_{j_h} \right) \prod_{T \in C_3} \left\{ \begin{matrix} j_{T_1} & j_{T_2} & j_{T_3} \\ j_{T_4} & j_{T_5} & j_{T_6} \end{matrix} \right\}. \quad (4.32)$$

The right hand side of eq. (4.32) is nothing but the partition function of the Ponzano–Regge model (4.18). Furthermore, since the Ponzano–Regge model is equivalent to the classical limit ($k \rightarrow \infty$) of the $ISO(3)$ Chern-Simon-Witten theory [5,24,25], we conclude

$$Z(L) = Z_{\text{PR}}(L) = Z_{\text{CSW}}(\mathcal{M}) \Big|_{(k=\infty)}, \quad (4.33)$$

where \mathcal{M} is a manifold with tetrahedral decomposition L .

5. Conclusions and Questions

We have defined a general class of three-dimensional topological lattice field theories, and shown that they are in one-to-one correspondence with Hopf algebras with antipode

$S = \frac{1}{\Lambda_0} T$. For the Hopf algebra $\mathbf{C}[G]$, we were able to show that the corresponding TLFT is equivalent to the lattice gauge theory with gauge group G at zero coupling. Furthermore, for $G = \text{SU}(2)$, the TLFT was also equivalent to the theory of Ponzano and Regge.

A number of questions are suggested by our results. Perhaps the most obvious is, how are our TLFTs related to other known topological theories in three dimensions, both on the lattice and in continuum? For example, the Ponzano–Regge theory, and hence the TLFT with $H = \mathbf{C}[\text{SU}(2)]$, is known to be equivalent to the continuum Chern–Simons–Witten theory with gauge group $ISO(3)$ [24,25]. We may conjecture that the CSW for the general inhomogeneous Lie group IG is equivalent to the TLFT with $H = \mathbf{C}[G]$. But that only begs the question: what TLFT is equivalent to CSW with arbitrary gauge group G ?

The Ponzano–Regge theory is the classical limit of the topological lattice theory of Turaev and Viro based on the quantum group $SU_q(2)$. Because $SU_q(2)$ is a Hopf algebra, one might expect the Turaev–Viro theory to be equivalent to the TLFT for $H = SU_q(2)$. However, because $S^2 \neq 1$, this Hopf algebra does not obey our constraint (except for $q = \pm 1$), so either we should look for another Hopf algebra or for a way to relax the constraint. The latter approach would require a generalization of our ansatz for three-dimensional lattice field theories.

One simple generalization of our ansatz, suggested by ref. [22], would be to assign colors to faces as well as to links. Consider, for example, a theory in which only the faces are colored. Given a colored tetrahedral lattice, we can assign a weight C_{xyzw} to each tetrahedron, a function of the colors x , y , z , and w on its four faces (ordered with a canonical orientation). The partition function is then the product over all tetrahedral cells of the weights, with indices contracted using a face–gluing operator g^{xy} . Topological invariance (restricted to tetrahedral lattices) is equivalent to invariance under the (2,3) and bubble moves, which are represented, respectively, by the following conditions on the weights:

$$C_{xyz}{}^u C_{urst} = C_{uxr}{}^v C_{wys}{}^u C_{ztv}{}^w \quad (5.1)$$

$$C_x{}^{uvw} C_{wvuy} = g_{xy} \quad (5.2)$$

Proceeding as before, we can treat the $C_{xyz}{}^w$ as structure constants for an algebraic structure with a “triple multiplication,” a trilinear map $m : A \otimes A \otimes A \rightarrow A$. Such structures are known as triple systems and have been extensively studied [32], but to our knowledge no study has been made of triple systems subject to the constraints (5.1) and (5.2).

Another obvious direction for future work is to study TLFTs in higher dimensions. The extension from two to three dimensions that we have presented suggests that the most straightforward generalization to D dimensions would be the following: First we regard a lattice as consisting of $(D - 1)$ -simplicies glued along $(D - 2)$ -dimensional hinges with $(D - 2)$ -dimensional boundaries. We then color these boundaries, and assign local weights individually to both the $(D - 1)$ -simplicies and the hinges, as functions of the colorings on their boundaries. The partition function is thus defined as the product of all the local weights summed over all colorings. In fact, when $D = 3$, the TLFTs we have studied are based on lattices consisting of 2-simplicies (triangles) glued along hinges with 1-dimensional boundaries. Also, in the dual TLFTs in two dimensions discussed in subsec. 2.6, we assigned weights to 1-simplices (the dual of gluing operators) and to zero-dimensional hinges (trivalent vertices, *i.e.*, the dual of triangles) as functions of the colorings on their zero-dimensional boundaries.

Let us now consider a four-dimensional LFT, in which 2-simplices are colored and weights are assigned to 3-simplices, as well as to two-dimensional hinges. Then, just as before, the weight of a 3D tetrahedron C_{xyzw} is a function of the four colors on its boundary faces. Since any 3D polyhedron can be decomposed into 3D tetrahedra, we can consistently define the weight of an arbitrary 3D polyhedron in terms of the C_{xyzw} , provided that eqs. (5.1) and (5.2) are satisfied. In this case, the tetrahedral weights C_{xyzw} again define a constrained triple system. On the other hand, the hinge operator in this LFT glues 3D tetrahedra together on 2-simplices. We denote the weight for a trivalent hinge with colors x , y and z by Δ^{xyz} , and glue together these trivalent hinges using h_{xy} in order to build up n -valent hinges. As in Sec. 3, the consistency of this construction will again require the Δ_x^{yz} to define a cosemisimple coassociative coalgebra. We suspect that the four-dimensional topological lattice model studied by Ooguri [33] is related to a theory of this type. It will be interesting to see whether such extensions to higher-dimensional theories will prove to be as rich in structure as 2D and 3D TLFTs.

Acknowledgements

It is a pleasure to thank J. Distler, S. Hosono, H. Kawai, A. LeClair, G. Moore, R. Myers, H. Ooguri, R. Plesser, M. Rocek, S.-H. H. Tye, T. Ward and B. Zumino for stimulating discussions. This work was supported in part by the National Science Foundation.

Appendix A. Brief Review of Hopf Algebras

In this appendix, we briefly review the basic structure of Hopf algebras [29]. We also prove several theorems used in sec. 3.

A.1. Algebra $(H; m, u)$

A vector space H over \mathbf{C} is called an **algebra** if the two (bi-) linear maps

$$(1) \text{ multiplication; } m : H \otimes H \longrightarrow H \quad (\text{A.1})$$

$$(2) \text{ unit; } u : \mathbf{C} \longrightarrow H \quad (\text{A.2})$$

satisfy the following commutative diagrams:

(i) associativity:

$$\begin{array}{ccc} H \otimes H \otimes H & \xrightarrow{m \otimes 1} & H \otimes H \\ \downarrow 1 \otimes m & & \downarrow m \\ H \otimes H & \xrightarrow{m} & H \end{array} \quad (\text{A.3})$$

(ii) unit:

$$\begin{array}{ccccc} \mathbf{C} \otimes H & \xrightarrow{u \otimes 1} & H \otimes H & \xleftarrow{1 \otimes u} & H \otimes \mathbf{C} \\ \searrow \sim & & \downarrow m & & \sim \swarrow \\ & & H & & \end{array} \quad (\text{A.4})$$

If we denote $m(\phi \otimes \phi')$ by $\phi \cdot \phi'$, and $u(1)$ by 1_H , then eqs. (A.3) and (A.4) are expressed, respectively, as

$$(\phi \cdot \phi') \cdot \phi'' = \phi \cdot (\phi' \cdot \phi'') \quad (\text{A.5})$$

$$1_H \cdot \phi = \phi = \phi \cdot 1_H. \quad (\text{A.6})$$

For later convenience, we fix a basis of H as $H = \bigoplus_{x \in X} \mathbf{C} \phi_x$, and introduce the structure constants $C_{xy}{}^z$ and u^x as

$$\phi_x \cdot \phi_y \ (\equiv m(\phi_x \otimes \phi_y)) = C_{xy}{}^z \phi_z \quad (\text{A.7})$$

$$1_H \ (\equiv u(1)) = u^x \phi_x \quad (\text{A.8})$$

where repeated indices are understood to be summed over. It is easy to show that eqs. (A.3) and (A.4) (or equivalently (A.5) and (A.6)) can be rewritten as

$$C_{xy}{}^u C_{uz}{}^w = C_{xu}{}^w C_{yz}{}^u \quad (\text{A.9})$$

$$u^x C_{xy}^z = \delta_y^z = C_{yx}^z u^x. \quad (\text{A.10})$$

The **metric** g_{xy} of the algebra is defined by

$$g_{xy} = C_{xu}^v C_{yv}^u, \quad (\text{A.11})$$

and the matrix (g_{xy}) is nondegenerate if and only if the algebra $(H; m, u)$ is semisimple (*i.e.* isomorphic to a direct sum of matrix rings) [12]. Furthermore, one can easily prove the following theorem:

Theorem A.1.

(a) $C_{xyz} \equiv C_{xy}^{z'} g_{z'z}$ is cyclically symmetric:

$$C_{xyz} = C_{yzx} = C_{zxy}. \quad (\text{A.12})$$

(b) For $u_z \equiv g_{zz'} u^{z'}$, we have

$$C_{xy}^z u_z = g_{xy}. \quad (\text{A.13})$$

(c) If H is semisimple, then u^x is uniquely determined by C_{xy}^z ;

$$u^x = g^{xx'} C_{x'u}^x, \quad (\text{A.14})$$

where (g^{xy}) is the inverse of (g_{xy}) ; $g^{xy} g_{yz} = \delta_z^x$.

A.2. Coalgebra $(H; \Delta, \epsilon)$

A vector space H over \mathbf{C} is called a **coalgebra** if the two (bi-) linear maps

$$(1') \text{ comultiplication; } \Delta : H \rightarrow H \otimes H \quad (\text{A.15})$$

$$(2') \text{ counit; } \epsilon : H \rightarrow \mathbf{C} \quad (\text{A.16})$$

satisfy the following commutative diagrams:

(i') coassociativity:

$$\begin{array}{ccc} H \otimes H \otimes H & \xrightarrow{\Delta \otimes 1} & H \otimes H \\ \uparrow 1 \otimes \Delta & & \uparrow \Delta \\ H \otimes H & \xleftarrow{\Delta} & H \end{array} \quad (\text{A.17})$$

(ii') counit:

$$\begin{array}{ccccc}
\mathbf{C} \otimes H & \xleftarrow{\epsilon \otimes 1} & H \otimes H & \xrightarrow{1 \otimes \epsilon} & H \otimes \mathbf{C} \\
& \swarrow \sim & \uparrow \Delta & \sim \searrow & \\
& & H & &
\end{array} \tag{A.18}$$

Fixing a basis of H as $H = \bigoplus_{x \in X} \mathbf{C} \phi_x$, and introducing the costructure constants Δ_x^{yz} and ϵ_x as

$$\Delta(\phi_x) = \Delta_x^{yz} \phi_y \otimes \phi_z \tag{A.19}$$

$$\epsilon(\phi_x) = \epsilon_x, \tag{A.20}$$

we can rewrite eqs. (A.17) and (A.18), respectively, as

$$\Delta_x^{yu} \Delta_u^{zw} = \Delta_x^{uw} \Delta_u^{yz} \tag{A.21}$$

$$\Delta_x^{yz} \epsilon_z = \delta_x^y = \epsilon_z \Delta_x^{zy}. \tag{A.22}$$

The **cometric** h^{xy} of the coalgebra is defined by

$$h^{xy} = \Delta_u^{vx} \Delta_v^{uy}. \tag{A.23}$$

These h^{xy} , Δ_x^{yz} , and ϵ_x obey the following theorem similar to Theorem A.1:

Theorem A.2.

(a') $\Delta^{xyz} \equiv h^{xx'} \Delta_{x'}^{yz}$ is cyclically symmetric:

$$\Delta^{xyz} = \Delta^{yzx} = \Delta^{zxy}. \tag{A.24}$$

(b') For $\epsilon^x \equiv h^{xx'} \epsilon_{x'}$, we have

$$\epsilon^x \Delta_x^{yz} = h^{yz}. \tag{A.25}$$

(c') If (h^{xy}) is nondegenerate, then ϵ_x is uniquely determined by Δ_x^{yz} ;

$$\epsilon_x = \Delta_u^{ux'} h_{x'x}, \tag{A.26}$$

where (h_{xy}) is the inverse of (h^{xy}) ; $h^{xy} h_{yz} = \delta_z^x$.

Note that, given an algebra $(H; m, u)$, we can always construct a coalgebra $(\tilde{H}; \tilde{\Delta}, \tilde{\epsilon})$. In fact, if we introduce $\tilde{H} \equiv \bigoplus_{x \in X} \mathbf{C} \phi^x$, and define the comultiplication $\tilde{\Delta}: \tilde{H} \rightarrow \tilde{H} \otimes \tilde{H}$ and the counit $\tilde{\epsilon}: \tilde{H} \rightarrow \mathbf{C}$ as

$$\tilde{\Delta}(\phi^x) \equiv C_{yz}^x \phi^y \otimes \phi^z \tag{A.27}$$

$$\tilde{\epsilon}(\phi^x) \equiv u^x. \tag{A.28}$$

then, as is easily shown, the associativity and unit conditions for the algebra H imply the coassociativity and counit conditions for the coalgebra \tilde{H} .

Similarly, we can construct an algebra $(\tilde{H}; \tilde{m}, \tilde{u})$ from a given coalgebra $(H; \Delta, \epsilon)$ as

$$\tilde{H} = \bigoplus_{x \in X} \mathbf{C}\phi^x \quad (\text{A.29})$$

$$\tilde{m}(\phi^x \otimes \phi^y) \equiv \Delta_z^{xy} \phi^z \quad (\text{A.30})$$

$$\tilde{u}(\phi^x) \equiv \epsilon_x \phi^x, \quad (\text{A.31})$$

A.3. Bialgebra $(H; m, u, \Delta, \epsilon)$

Suppose that a vector space H is an algebra with respect to (m, u) and also a coalgebra with respect to (Δ, ϵ) . Then we can prove [29]

Theorem A.3. *The following statements are equivalent:*

- (i) m and u are coalgebra morphisms with respect to (Δ, ϵ) .
- (ii) Δ and ϵ are algebra morphisms with respect to (m, u) .

In fact, each of these statements is equivalent to the following set of four conditions:

$$\Delta \circ m = (m \otimes m) \circ (1 \otimes \tau \otimes 1) \circ (\Delta \otimes \Delta) \quad (\text{A.32})$$

$$\Delta \circ u = u \otimes u \quad (\text{A.33})$$

$$\epsilon \circ m = \epsilon \otimes \epsilon \quad (\text{A.34})$$

$$\epsilon \circ u = 1, \quad (\text{A.35})$$

where τ is the twist mapping, $\tau : H \otimes H \ni \phi \otimes \phi' \mapsto \phi' \otimes \phi \in H \otimes H$. In terms of the basis $\{\phi_x; x \in X\}$, these equations become

$$C_{xy}^z \Delta_z^{ab} = \Delta_x^{pq} \Delta_y^{rs} C_{pr}^a C_{qs}^b \quad (\text{A.36})$$

$$u^x \Delta_x^{yz} = u^y u^z \quad (\text{A.37})$$

$$C_{xy}^z \epsilon_z = \epsilon_x \epsilon_y \quad (\text{A.38})$$

$$\epsilon_x u^x = 1. \quad (\text{A.39})$$

The quintet $(H; m, u, \Delta, \epsilon)$ is called a **bialgebra** if either of the two equivalent conditions in Theorem A.3 is satisfied. Note that the quintet $(\tilde{H}; \tilde{m}, \tilde{u}, \tilde{\Delta}, \tilde{\epsilon})$ as defined at the end of subsection A.2 is also a bialgebra if (and only if) $(H; m, u, \Delta, \epsilon)$ is a bialgebra.

A.4. Hopf algebra $(H; m, u, \Delta, \epsilon, S)$

Let $(H; m, u, \Delta, \epsilon)$ be a bialgebra. If a linear map $S : H \rightarrow H$ satisfies the following equation

$$m \circ (1 \otimes S) \circ \Delta = m \circ (S \otimes 1) \circ \Delta = u \circ \epsilon, \quad (\text{A.40})$$

then the sextet $(H; m, u, \Delta, \epsilon, S)$ is said to be a **Hopf algebra** with antipode S . With respect to our usual basis, eq. (A.40) may be expressed as

$$\Delta_x^{ab} S_b^c C_{ac}^y = \Delta_x^{ab} S_a^c C_{cb}^y = u^y \epsilon_x \quad (\text{A.41})$$

with $S(\phi_x) = S^y_x \phi_y$.

For the antipode S , we have the following two important theorems [29]:

Theorem A.4. *The antipode S is unique if it exists. Furthermore, S is an algebra antimorphism with respect to (m, u) :*

$$(i) \quad S \circ m = m \circ (S \otimes S) \circ \tau, \text{ i.e.}$$

$$S(\phi \cdot \phi') = S(\phi') \cdot S(\phi) \quad \text{for } \phi, \phi' \in H \quad (\text{A.42})$$

$$(ii) \quad S \circ u = u, \text{ i.e.}$$

$$S(1_H) = 1_H, \quad (\text{A.43})$$

and S is also a coalgebra antimorphism with respect to (Δ, ϵ) :

$$(iii) \quad \Delta \circ S = \tau \circ (S \otimes S) \circ \Delta \quad (\text{A.44})$$

$$(iv) \quad \epsilon \circ S = \epsilon. \quad (\text{A.45})$$

These equations (A.42)–(A.45) can be rewritten in terms of the basis $\{\phi_x; x \in X\}$, as follows:

$$(i') \quad S^z_{z'} C_{yx}^{z'} = C_{x'y'}^z S^{x'}_x S^{y'}_y \quad (\text{A.46})$$

$$(ii') \quad S^x_y u^y = u^x \quad (\text{A.47})$$

$$(iii') \quad \Delta_{x'}^{zy} S^{x'}_x = S^y_{y'} S^z_{z'} \Delta_x^{y'z'} \quad (\text{A.48})$$

$$(iv') \quad \epsilon_x S^x_y = \epsilon_y. \quad (\text{A.49})$$

Theorem A.5. *The following conditions on the antipode $S = (S^x_y)$ are equivalent:*

$$(i) \quad S^2 = 1 \quad (A.50)$$

$$(ii) \quad \Delta_x^{ab} S^c_b C_{ca}^y = u^y \epsilon_x \quad (A.51)$$

$$(iii) \quad \Delta_x^{ab} S^c_a C_{bc}^y = u^y \epsilon_x . \quad (A.52)$$

An immediate consequence is the following:

Corollary A.6. *If the Hopf algebra $(H; m, u, \Delta, \epsilon, S)$ is commutative ($C_{xy}^z = C_{yx}^z$) or cocommutative ($\Delta_x^{yz} = \Delta_x^{zy}$), then $S^2 = 1$.*

We make one final remark concerning Hopf algebras: if $(H; m, u, \Delta, \epsilon, S)$ is a Hopf algebra, then $(\tilde{H}; \tilde{m}, \tilde{u}, \tilde{\Delta}, \tilde{\epsilon}, \tilde{S} \equiv {}^t S)$ is also a Hopf algebra, and is called the **dual Hopf algebra**. Here, ${}^t S$ is the transpose of S ; ${}^t S(\phi^x) = S^x_y \phi^y$ for $\phi^x \in \tilde{H}$.

A.5. Properties of the Operator T Following from the Constraint (3.21)

Let $T : H \ni \phi_y \mapsto \phi_x T^x_y \in H$ be a linear map with $T^x_y \equiv h^{xz} g_{zy}$, and let Λ_0 be a numerical constant defined by

$$\Lambda_0 \equiv \epsilon_x T^x_y u^y = \epsilon^x u_x . \quad (A.53)$$

Then, we have

Theorem A.7. *For a bialgebra $(H; m, u, \Delta, \epsilon)$, the following statements are equivalent:*

(a) *T satisfies the equation (eq. (3.21))*

$$\Lambda T^z_y \Delta_z^{ba} = T^a_r T^b_s \Delta_y^{rs} \quad (A.54)$$

for a numerical constant Λ .

(b) *T satisfies the equations*

$$T^x_y u^y = \Lambda_1 u^x \quad (\Leftrightarrow h^{xy} u_y = \Lambda_1 u^x) \quad (A.55)$$

$$\epsilon_x T^x_y = \Lambda_2 \epsilon_y \quad (\Leftrightarrow \epsilon^x g_{xy} = \Lambda_2 \epsilon_y) \quad (A.56)$$

for numerical constants Λ_1 and Λ_2 .

(c) *The bialgebra is enhanced to a Hopf algebra with the antipode*

$$S = \frac{1}{\Lambda_3} T \quad (A.57)$$

for a numerical constant Λ_3 .

Furthermore, if (a), (b), or (c) is satisfied, these numerical constants Λ , Λ_1 , Λ_2 , and Λ_3 are all equal to Λ_0 , and the antipode S in (c) satisfies

$$S^2 = 1. \quad (\text{A.58})$$

Proof. (a) \Rightarrow (b) : Eq. (A.55) can be shown as follows: We first rewrite eq. (A.54) as

$$\Lambda g_{yz} \Delta^{zba} = T^a_r T^b_s \Delta_y^{rs}, \quad (\text{A.59})$$

and multiply this by $h_{ac} u^c u^y$. Then, by using eq. (A.37) we have

$$\Lambda u^2 u^b = u^2 T^b_s u^s \quad (u^2 \equiv u^x u_x). \quad (\text{A.60})$$

Since u^2 is not zero in general, we conclude $\Lambda u^b = T^b_s u^s$. Eq. (A.56) can be obtained just by multiplying eq. (A.54) by $\epsilon_a \epsilon_c (T^{-1})^c_b$. Note that $\Lambda_1 = \Lambda_2 = \Lambda$.

(b) \Rightarrow (c) : We first note that $\Lambda_1 = \Lambda_2 = \Lambda_0$ since $\epsilon_x u^x = 1$ by eq. (A.39). We then multiply eq. (A.36) by $\epsilon^x u_a$, and obtain

$$\Lambda_0 \epsilon_y u^b = \Delta_y^{rs} T^q_r C_{qs}^b \quad (\text{A.61})$$

or

$$\epsilon_x u^y = \Delta_x^{ab} \left(\frac{1}{\Lambda_0} T^c_a \right) C_{cb}^y. \quad (\text{A.62})$$

Similarly, by multiplying $\epsilon^y u_b$, we obtain

$$\Lambda_0 \epsilon_x u^a = \Delta_x^{pq} T^r_q C_{pr}^a \quad (\text{A.63})$$

or

$$\epsilon_x u^y = \Delta_x^{ab} \left(\frac{1}{\Lambda_0} T^c_b \right) C_{ac}^y. \quad (\text{A.64})$$

Eqs. (A.62) and (A.64) imply that $\frac{1}{\Lambda_0} T$ satisfies the axiom of antipode (see eq. (A.41)). By using the uniqueness of the antipode as stated in Theorem A.4, we conclude that the bialgebra can be enhanced to a Hopf algebra with antipode $S = \frac{1}{\Lambda_0} T$.

(c) \Rightarrow (a) : Due to Theorem A.4, $S = \frac{1}{\Lambda_3} T$ is a coalgebra antimorphism. This is exactly the statement (a) with $\Lambda = \Lambda_3 = \Lambda_0$.

Finally, to prove that $S^2 = 1$ (or equivalently $T^2 = \Lambda_0^2$), we multiply eq. (A.54) by $\epsilon^y h_{bc}$, and rewrite eq. (A.56) in the form $T^x_y \epsilon^y = \Lambda_2 \epsilon^x = \Lambda_0 \epsilon^x$. Then,

$$\begin{aligned} \Lambda_0^2 \delta_c^a &= h_{bc} T^a_r T^b_s h^{rs} \\ &= T^a_r h_{bc} h^{bd} g_{ds} h^{rs} \\ &= T^a_r T^r_c. \quad (\text{QED}) \end{aligned} \quad (\text{A.65})$$

Appendix B. Proof of Eq. (3.20) and Derivation of the Bubble and (2,3) Moves

B.1. Proof of Eq. (3.20)

Lemma B.1.

$$\begin{aligned} u^x \Delta_x^{pq} &= u^p u^q \\ C_{xy}^z \epsilon_z &= \epsilon_x \epsilon_y \end{aligned} \tag{B.1}$$

Proof. We prove this equation by first attaching two triangles C_{pab} and C_{qcd} to $u^x \Delta_x^{pq}$, as shown in Fig. B-1a,b. We then shrink the shaded region in Fig. B-1b and obtain Fig. B-1c. Topological invariance requires

$$u^x \Delta_x^{pq} C_{pab} C_{qcd} = g_{ab} g_{cd} = u^p C_{pab} u^q C_{qcd}, \tag{B.2}$$

where we have used eq. (3.10). Since eq. (B.2) holds for arbitrary triangles, C_{pab} and C_{qcd} , the first half of Lemma B.1 follows. We prove the second part by going to the dual lattice and using the first part of the proof. (QED)

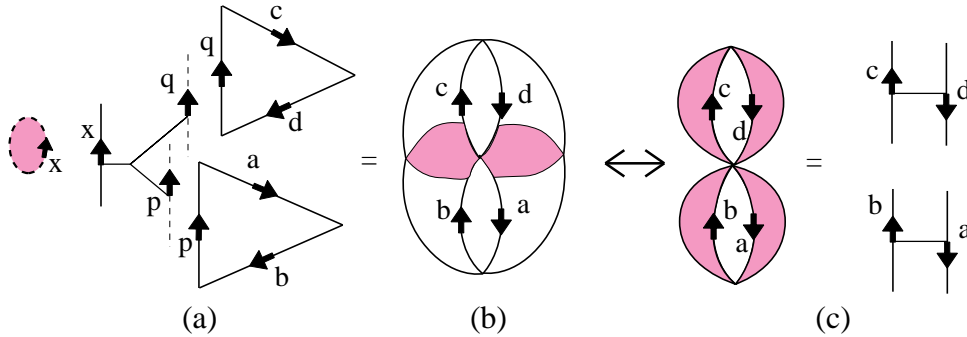


Fig. B-1: Proof of Lemma B.1.

B.2. Derivation of the Bubble Move

In this subsection, we will prove the invariance under the bubble move, assuming only that the hinge equation is satisfied.

Lemma B.2. *The configuration shown in Fig. B-2a, consisting of two triangles sharing three edges, is equivalent to the single triangle appearing in Fig. B-2b.*

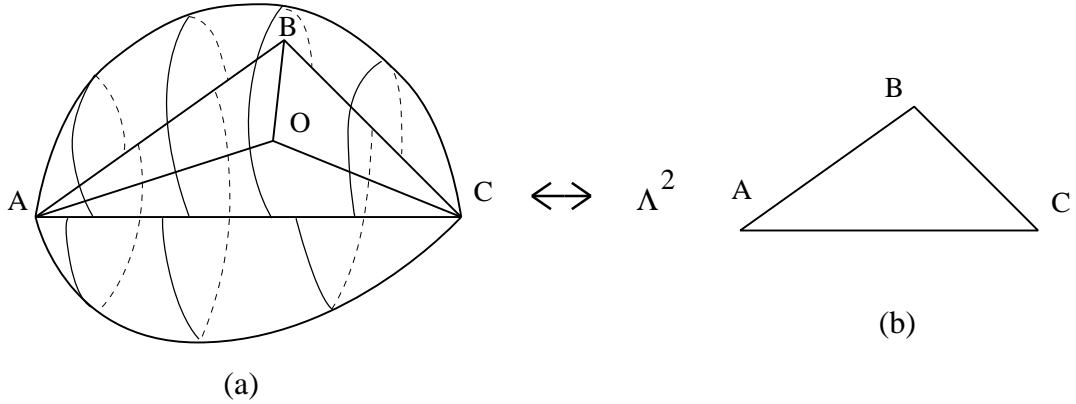


Fig. B-4: Bubble move.

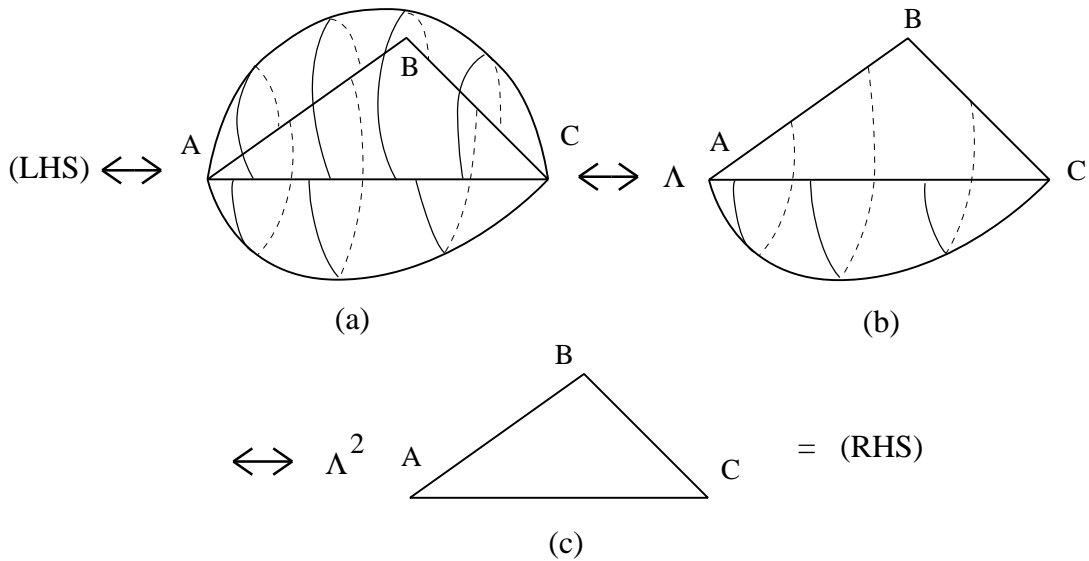


Fig. B-5: Derivation of the bubble move.

In Fig. B-4a, there are total of five triangles. Two of them are determined by the vertices ABC , and share the three edges \overline{AB} , \overline{BC} and \overline{CA} . They are described by the two curved surfaces in the upper and the lower parts of the figure. The other three triangles are determined by the vertices ABO , ACO and BCO .

Proof: We first perform a 2D (1,3) move to replace the three internal triangles ABO , ACO and BCO by a single triangle ABC (see Fig. B-5a). Then we apply Lemma B.2 twice and obtain Fig. B-5c. (QED)

Corollary B.4. *The configuration of four triangles linked together as in Fig. B-6a is equivalent to the pair of triangles shown in Fig. B-6b.*

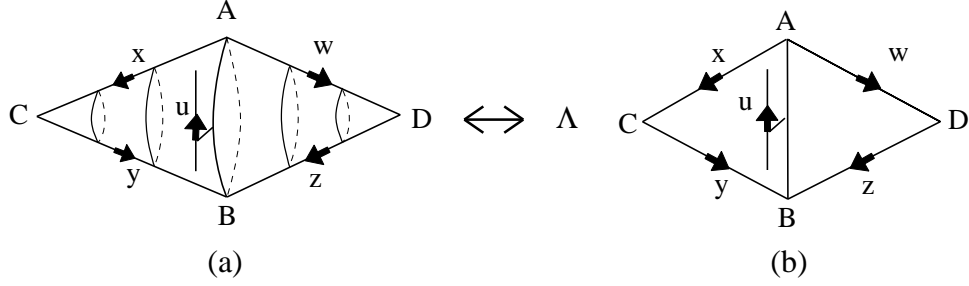


Fig. B-6: Corollary B.4.

To be more precise, we describe in words how these four triangles are connected (see also Fig. B-7a). The two triangles with vertices ABC share edges \overline{AC} and \overline{BC} ; the other two determined by ABD join along \overline{AD} and \overline{BD} . The two front triangles are connected by a 3-hinge operator along the solid edge \overline{AB} . The two rear triangles are connected by a 2-hinge operator along the dotted line \overline{AB} .

Proof. By applying the hinge move to the two triangles with vertices ABC in Fig. B-7b, we obtain Fig. B-7c, which contains three different hinges, g^{bc} , Δ_u^{da} , and $\Delta^{b''e}_a S^{b'}_{b''} h_{bb'}$ (where e denotes the edge variable of the triangle C_{exy}). These three hinge operators can be simplified using eq. (3.18)

$$\begin{aligned}
 g^{bc} \Delta_u^{da} \Delta^{b''e}_a S^{b'}_{b''} h_{bb'} &= g^{bc} \Delta_u^{da} \Delta^{b''e}_a \left(\frac{1}{\Lambda} h^{b'w} g_{wb''} h_{bb'} \right) \\
 &= \frac{1}{\Lambda} \Delta_u^{da} \Delta^{ce}_a = \frac{1}{\Lambda} \Delta_u^{dce},
 \end{aligned} \tag{B.4}$$

which is exactly the 4-hinge operator connecting the four triangles along the edge \overline{AB} in Fig. B-7d. We then apply Lemma B.2 to obtain Fig. B-7e. (QED)

B.3. Derivation of the (2,3) Move

In this subsection, we will prove the invariance under the (2,3) move, with the assumption that the hinge equation is satisfied.

Lemma B.5. *The configuration of four triangles in Fig. B-8a is equivalent to the three triangles in Fig. B-8b.*

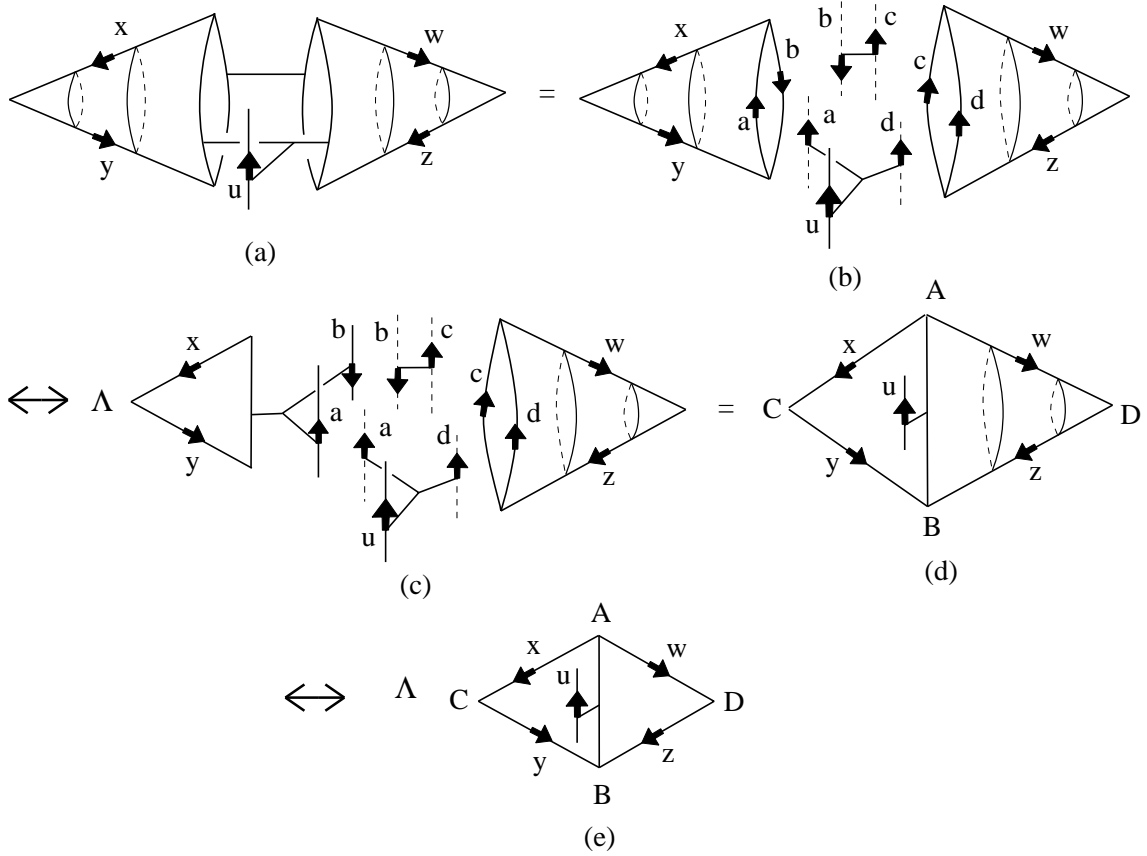


Fig. B-7: Proof of Corollary B.4.

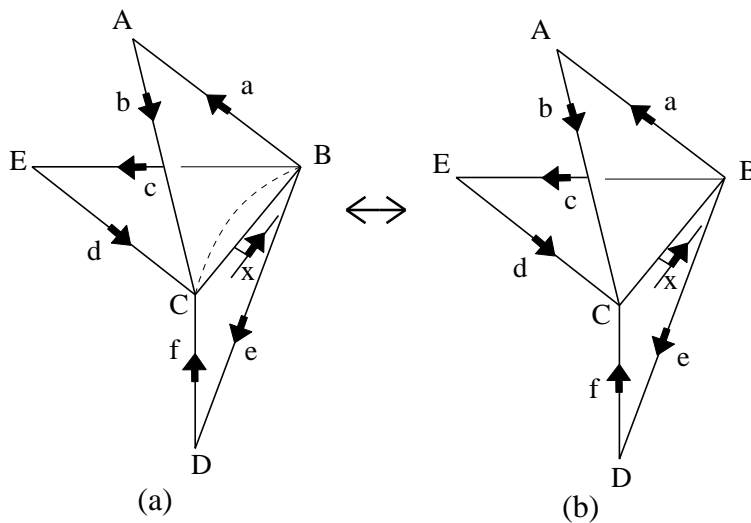


Fig. B-8: Lemma B.5.

The two triangles determined by vertices BCD share the two edges \overline{BD} and \overline{CD} . One

of these two triangles is connected to the triangle BCE by a 2-hinge operator along the dotted line \overline{BC} . The other triangle is linked to ABC by a 3-hinge operator along the solid line \overline{BC} .

Proof. We apply the hinge move to the two triangles BCD in Fig. B-8a. The resulting hinges can be manipulated in a similar way shown in eq. (B.4) to yield the hinge needed in Fig. B-8b. (QED)

Lemma B.6. *The three triangles join along a 3-hinge, as shown in Fig. B-9a, is equivalent to the configurations of four triangles shown in Fig. B-9b and Fig. B-9c.*

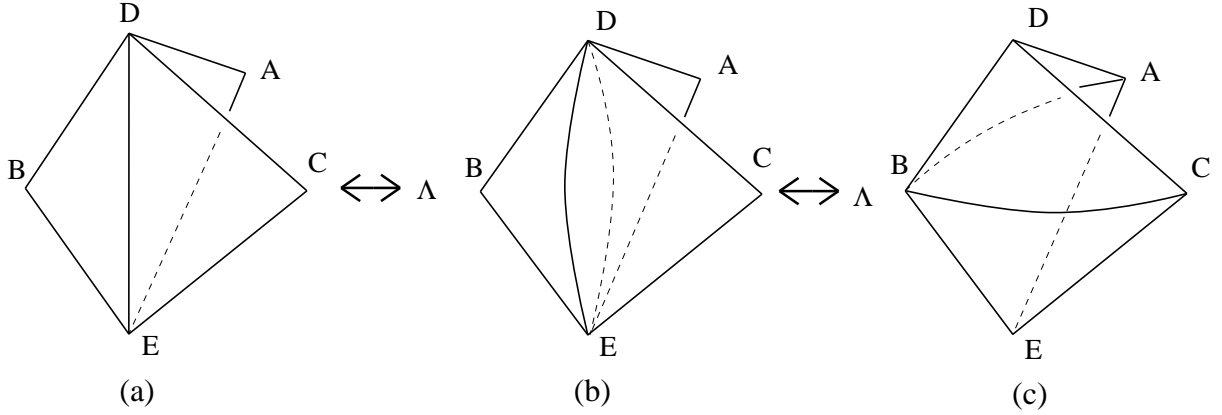


Fig. B-9: The change of three triangles joining along a 3-hinge.

Proof. We first decompose the three triangles in Fig. B-9a (or Fig. B-10a), into the configuration in Fig. B-10b. The hinge shown in Fig. B-10b can be written as

$$\begin{aligned} \Delta^{vz'w'} S_{z'}^z S_{w'}^w &= \Delta^{vz'w'} S_{z'}^{-1z} S_{w'}^{-1w} = \Delta^{vz'w'} \Lambda^2 g^{zy} h_{yz'} g^{wx} h_{xw'} \\ &= \Lambda^2 \Delta_{yx}^v g^{zy} g^{wx}, \end{aligned} \quad (\text{B.5})$$

where we have used the property $S^2 = 1$, *i.e.*, $S = S^{-1}$. $\Delta_{yx}^v g^{zy} g^{wx}$ are just the hinges needed in Fig. B-10c. By inflating the left triangles in Fig. B-10c with the hinge move and connecting the resulting triangles by the 2-hinge operators, g^{zy} and g^{wx} , we obtain Fig. B-10e. Then we can apply twice the (2,2) move to obtain Fig. B-9c. (QED)

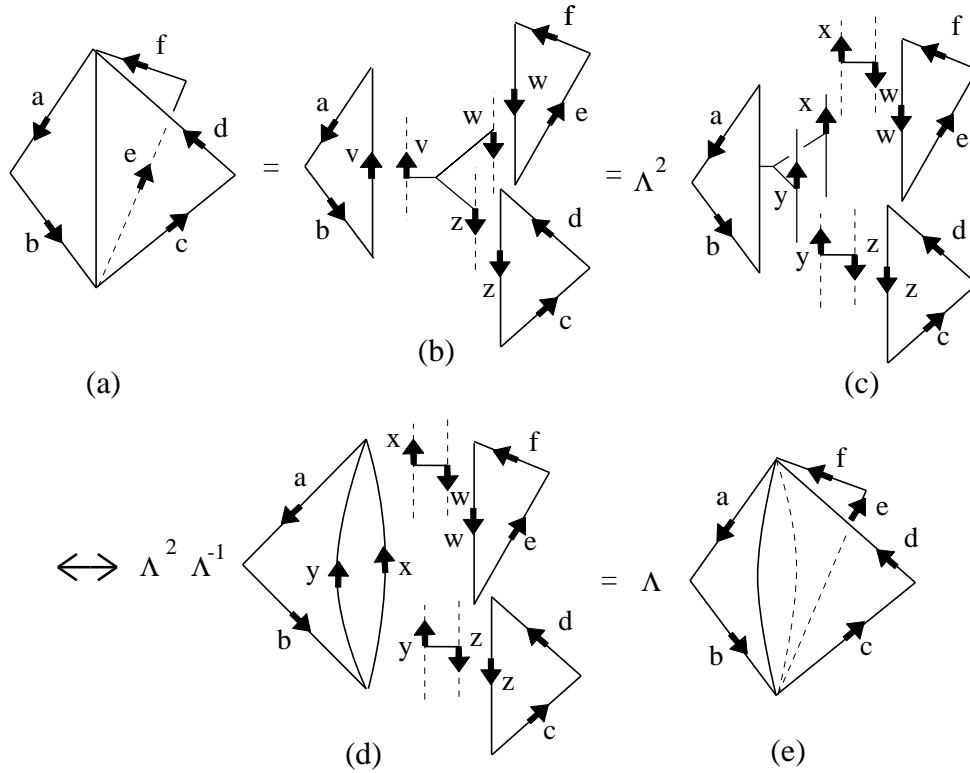


Fig. B-10: The process from Fig. B-9a to Fig. B-9b.

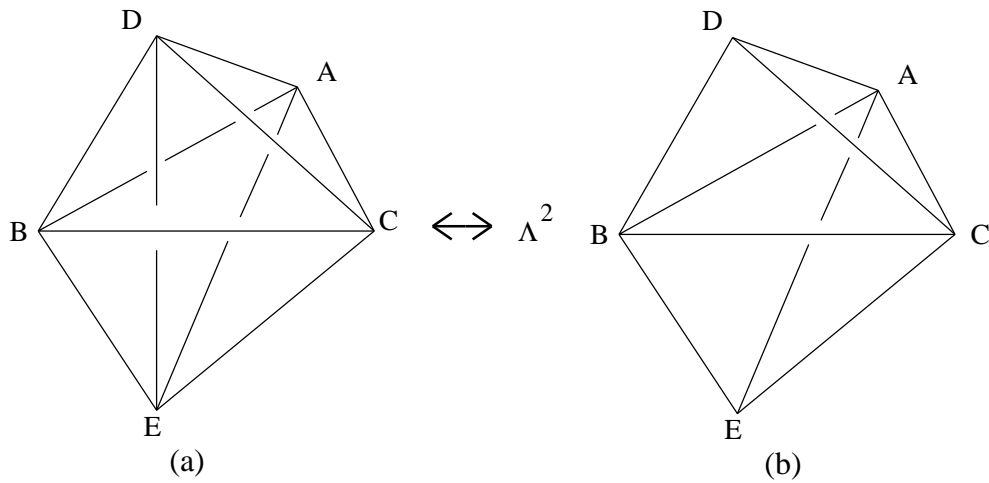


Fig. B-11: (2,3) move.

Theorem B.7. ((2,3) move): *The configuration of three tetrahedra sharing a single edge in Fig. B-11a is equivalent to two tetrahedra with a common face as in Fig. B-11b.*

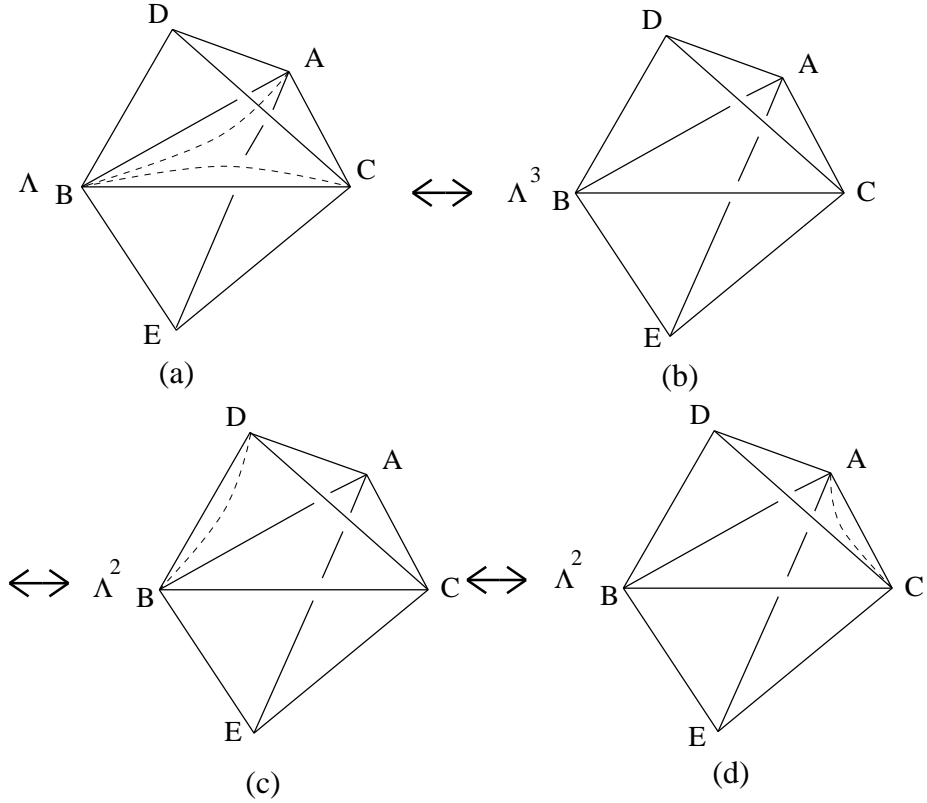


Fig. B-12: Proof of (2,3) move.

Proof. We first replace the three internal triangles in Fig. B-12a by four triangles in Fig. B-9c using Lemma B.6. The resulting four internal triangles in Fig. B-9c are connected to the original external faces according to Fig. B-12a. Next, we apply Lemma B.4 to deflate the internal triangles and obtain a single polyhedron with six faces shown in Fig. B-12b. Again, we use Lemma B.4 to inflate the pair of triangles CBD and BAD , leading to the configuration of Fig. B-12c. In Fig. B-12c, the two internal triangles are glued along the dotted line \overline{BD} with a 2-hinge operator. Then, we apply the (2,2) move to the two internal triangles to obtain Fig. B-12d, where the dotted line \overline{BD} has been replaced by the dotted line \overline{AC} . Finally, we use Lemma B.5 to collapse the two triangles ADC to a single triangle. This results in the configuration shown in Fig. B-11b, in which the two tetrahedra meet on the face ABC . (QED)

References

- [1] E. Witten: *Nucl. Phys.* **B311** (1988) 46.
- [2] G. Moore and N. Seiberg: *Phys. Lett.* **B220** (1989) 422.
- [3] E. Witten: *Nucl. Phys.* **B322** (1989) 629; E. Witten, *Nucl. Phys.* **B330** (1990) 285.
- [4] E. Witten: *Nucl. Phys.* **B268** (1986) 253; E. Witten, IAS preprint IASSNS-HEP-92-45, hep-th/9207094.
- [5] E. Witten: *Commun. Math. Phys.* **121** (1989) 351.
- [6] E. Witten: *Commun. Math. Phys.* **117** (1988) 353.
- [7] E. Witten: *Nucl. Phys.* **B340** (1990) 281.
- [8] M. Kontsevich: *Commun. Math. Phys.* **147** (1993) 1.
- [9] J.F. Wheeler: *Phys. Lett.* **223B** (1989) 451.
- [10] T. Jönsson: *Phys. Lett.* **265B** (1991) 141.
- [11] C. Bachas and P.M.S. Petropoulos: *Commun. Math. Phys.* **152** (1993) 191.
- [12] M. Fukuma, S. Hosono and H. Kawai: Lattice topological field theory in two-dimensions, Cornell preprint CLNS 92/1173, hep-th/9212154.
- [13] M. Gross and S. Varsted: *Nucl. Phys.* **B378** (1992) 367.
- [14] D. Boulatov: *Mod. Phys. Lett.* **A7** (1992) 1629.
- [15] A. Migdal: *Sov. Phys. J.E.T.P.* **42** (1975) 413.
- [16] T. Eguchi and S.K. Yang: *Mod. Phys. Lett.* **A5** (1991) 1693.
- [17] G. Ponzano and T. Regge: in Bloch, F. (ed.) *Spectroscopic and Group Theoretical Methods in Physics*. Amsterdam: North-Holland 1968.
- [18] V.G. Turaev and O.Y. Viro: *Topology* **31** (1992) 865.
- [19] S. Mizoguchi and T. Tada: *Phys. Rev. Lett.* **68** (1992) 1795; F. Archer and R.M. Williams: *Phys. Lett.* **B273** (1991) 438.
- [20] B. Durhuus, H.P. Jakobsen and R. Nest: *Nucl. Phys. B* **25A** (*Proc. Suppl.*) (1992) 109.
- [21] F.J. Archer: *Phys. Lett.* **295B** (1992) 199.
- [22] G. Felder and O. Grandjean: On combinatorial three-manifold invariants, ETH preprint, 1992.
- [23] R. Dijkgraaf and E. Witten: *Commun. Math. Phys.* **129** (1990) 393.
- [24] V.G. Turaev: Quantum invariants of 3-manifolds, Strasbourg preprint ISSN 0755-3390.
- [25] H. Ooguri and N. Sasakura: *Mod. Phys. Lett.* **A6** (1991) 3591; H. Ooguri, *Nucl. Phys.* **B382** (1992) 276.
- [26] J.W. Alexander: *Ann. Math.* **31** (1930) 292.
- [27] E. Witten: *Commun. Math. Phys.* **141** (1991) 435; *J. Geometry and Phys.* **9** (1992) 303.
- [28] M. Atiyah: *Publ. Math. IHES* **68** (1988) 175.

- [29] E. Abe: *Hopf algebras*. Cambridge: Cambridge University Press 1980.
- [30] M. Creutz: *Quarks, Gluons and Lattice*. Cambridge: Cambridge University Press, 1983.
- [31] A. Messiah: *Quantum Mechanics*, Vol. **II**. Amsterdam: North-Holland 1962.
- [32] E. Neher: *Jordan triple systems by the grid approach, Lecture Notes in Mathematics*. Berlin: Springer-Verlag, 1987.
- [33] H. Ooguri: *Mod. Phys. Lett.* **A7** (1992) 2799.